

Mechanistic understanding of biogenic Mn-oxide mediated bisphenol A degradation

by

Nusrat Shobnam

B.S., Bangladesh University of Engineering and Technology, 2016

A THESIS

submitted in partial fulfillment of the requirements for the degree

MASTER OF SCIENCE

Department of Civil Engineering  
Carl R. Ice College of Engineering

KANSAS STATE UNIVERSITY  
Manhattan, Kansas

2020

Approved by:

Major Professor  
Dr. Jeongdae Im

# **Copyright**

© Nusrat Shobnam 2020.

## Abstract

Bisphenol A (BPA) is a monomer of polycarbonate plastic which is produced in a large volume. The environmental fate of BPA has been of great concern due to its estrogenic properties. BPA had been considered recalcitrant under anoxic conditions, but recent studies showed that BPA is degraded by synthetic manganese oxides ( $\text{MnO}_{2\text{-syn}}$ ) without the requirement of oxygen. Manganese oxides ( $\text{MnO}_2$ ) is a naturally occurring, strong oxidant, and its formation is mainly attributed to microbial Mn(II) oxidation in the environment. However, the reactivity of biologically produced  $\text{MnO}_2$  ( $\text{MnO}_{2\text{-bio}}$ ) towards BPA has not been demonstrated.  $\text{MnO}_{2\text{-bio}}$  is the result of microbial Mn(II) oxidation to Mn(IV). This process involves two single-electron transfer reactions with Mn(III) as a transient intermediate, and generally prevails in nature as Mn(III) containing Mn(III/IV)-oxide. Mn(III) is also a strong oxidant and can contribute to the oxidation reaction of BPA. In this thesis, we first used three well-characterized Mn(II) oxidizing bacteria (MOB), *Roseobacter* sp. AzwK-3b, *Erythrobacter* sp. SD-21, and *Pseudomonas putida* GB-1 to determine if they can mediate BPA degradation by producing  $\text{MnO}_{2\text{-bio}}$ . Then, we examined the relative contribution of Mn(III) in BPA degradation by  $\text{MnO}_{2\text{-bio}}$ , using *R. AzwK-3b* as a model organism.

In the first study, we demonstrated that *R. AzwK-3b* and *E. SD-21* degraded BPA in absence of Mn(II) which has not been reported previously within these genera. In the presence of Mn(II), BPA degradation by the two strains became faster indicating  $\text{MnO}_{2\text{-bio}}$  enhanced BPA degradation. *P. putida* GB-1 did not degrade BPA in the absence of Mn(II), but BPA degradation was observed in the presence of Mn(II). For all three bacteria, high BPA degradation rates were observed with 10  $\mu\text{M}$  Mn(II) and BPA degradation decreased with increasing Mn(II) concentrations even though

more  $\text{MnO}_{2\text{-bio}}$  was formed with higher Mn(II) concentrations, suggesting that excess Mn(II) blocked the  $\text{MnO}_{2\text{-bio}}$  surface.

In the second study, we examined the relative role of Mn(III) in BPA degradation by  $\text{MnO}_{2\text{-bio}}$ .  $\text{MnO}_{2\text{-bio}}$  produced by *R. AzwK-3b* is a hexagonal-birnessite-like colloidal phase. This initial phase is known to undergo “aging” process and transforms into triclinic-birnessite-like particulate phase. We prepared two phases of  $\text{MnO}_{2\text{-bio}}$  (colloidal and particulate) and their synthetic counterparts (hexagonal and triclinic birnessite) and compared Mn(III) content, Mn(III) availability, and their impacts on BPA degradation rates. At neutral pH, both phases of  $\text{MnO}_{2\text{-bio}}$  did not show significant BPA degradation, but degradation occurred when a chelating agent, pyrophosphate, was added, suggesting that Mn(III) plays a major role in  $\text{MnO}_{2\text{-bio}}$  reactivities. The result was consistent with the high Mn(III) content in colloidal and particulate  $\text{MnO}_{2\text{-bio}}$  (64% and 62%, respectively). Relatively high Mn(III) content was observed in triclinic  $\text{MnO}_{2\text{-syn}}$  (36%), but BPA degradation rate was not as high as  $\text{MnO}_{2\text{-bio}}$ . We measured Mn(III) release rates of each  $\text{MnO}_2$ , and they showed high correlation with BPA degradation rates. Mn(III) release rates may account for accessible free Mn(III) from Mn(III)-pyrophosphate complex contributing to the higher BPA degradation rates. Combined, these results provide mechanistic understanding of Mn(III) containing Mn-oxides-mediated contaminant transformation that are relevant to natural and engineered environments.

# Table of Contents

List of Figures .....	vii
List of Tables .....	x
Acknowledgements .....	xi
Dedication .....	xii
Chapter 1 - Introduction .....	1
1.1 Goals and objectives .....	7
Chapter 2 - Biologically mediated abiotic degradation (BMAD) of bisphenol A by three Mn(II) oxidizing bacteria.....	8
2.1 Introduction.....	8
2.2 Materials and methods .....	9
2.2.1 Chemicals and preparation of MnO <sub>2-syn</sub> .....	9
2.2.2 BPA degradation by MOB with varying concentrations of Mn(II).....	9
2.2.3 Abiotic BPA degradation by MnO <sub>2-syn</sub> with and without Mn(II).....	10
2.2.4 Analytical procedures .....	11
2.3 Results.....	12
2.3.1 BPA degradation by MOB without Mn(II).....	12
2.3.2 BPA degradation by MOB with Mn(II).....	15
2.3.3 MnO <sub>2-bio</sub> formation in MOB in the absence of BPA.....	20

2.3.4 Effect of BPA on the growth of MOB .....	22
2.4 Discussion.....	25
2.5 Environmental implications .....	28
Chapter 3 - The relative roles of Mn(III) and Mn(IV) in BPA degradation by Mn-oxides.....	29
3.1 Introduction.....	29
3.2 Materials and Methods.....	30
3.2.1 Chemicals and MnO <sub>2</sub> preparation .....	30
3.2.2 Preparation of cell free biogenic MnO <sub>2-bio</sub> .....	30
3.2.3 Mn(III)-pyrophosphate complex preparation and measurement .....	31
3.2.4 Mn(III) extraction from MnO <sub>2-syn</sub> .....	32
3.2.5 BPA degradation kinetics.....	32
3.3 Results.....	33
3.3.1 Abiotic BPA degradation with cell free biogenic and synthetic MnO <sub>2</sub> .....	33
3.3.2 Mn (III) availability in different MnO <sub>2</sub> .....	38
3.3.3 BPA degradation by Mn(III) acetate -PP at different ligands and Mn(III) extracted from triclinic birnessite .....	41
3.4 Discussion.....	43
3.5 Environmental Implications.....	46
Chapter 4 - Conclusion .....	47
References.....	49

## List of Figures

Figure 1.1 Molecular structure of bisphenol A (BPA). .....	1
Figure 1.2 BPA degradation pathways and intermediates mediated by biological entities and reactive mineral phases demonstrated in the laboratory. (Im et al., 2016) .....	3
Figure 1.3 Microbial Mn(II) oxidation with different enzymatic systems in (a) <i>R. AzwK-3b</i> , (b) <i>E. SD-21</i> and <i>P. putida</i> GB-1, (c) <i>P. putida</i> GB-1.....	5
Figure 1.4 Mn(II) oxidation occurs via two single-electron transfer reactions with Mn(III) as a transient intermediate.....	6
Figure 2.1 BPA degradation (left column) and MnO <sub>2</sub> - <sub>bio</sub> formation (right column) at different MnCl <sub>2</sub> concentration for (a), (b) <i>R. AzwK-3b</i> , (c), (d) <i>E. SD-21</i> and (e), (f) <i>P. putida</i> GB-1. Error bars represent the standard deviation of triplicate samples. Error bars smaller than the symbol size are not depicted. ....	13
Figure 2.2 BPA degradation without Mn(II) in J acetate medium with <i>R. AzwK-3b</i> . Error bars represent the standard deviation of triplicate samples. Error bars smaller than the symbol size are not depicted. ....	14
Figure 2.3 BPA degradation in the presence and absence of inhibitor metyrapone with <i>E. SD-21</i> . Error bars represent the standard deviation of triplicate samples. Error bars smaller than the symbol size are not depicted. ....	15
Figure 2.4 BPA degradation vs MnO <sub>2</sub> formation at different MnCl <sub>2</sub> concentration for (a) <i>R. AzwK-3b</i> , (b) <i>E. SD-21</i> and (d) <i>P. putida</i> GB-1. Error bars represent the standard deviation of triplicate samples. Error bars smaller than the symbol size are not depicted. ....	17

Figure 2.5 BPA degradation in the presence and absence of 500  $\mu\text{M}$   $\text{MnCl}_2$  in solutions containing 44  $\mu\text{M}$  BPA and 2 mM  $\text{MnO}_{2\text{-syn}}$ . Error bars represent the standard deviation of triplicate samples. Error bars smaller than the symbol size are not depicted..... 18

Figure 2.6 HCA formation (left column) and conversion ratio from BPA to HCA (right column) for (a), (b) *R. AzwK-3b*, (c), (d) *E. SD-21* and (e), (f) *P. putida* GB-1 at different  $\text{MnCl}_2$  concentrations. Error bars represent the standard deviation of triplicate samples. Error bars smaller than the symbol size are not depicted..... 19

Figure 2.7 Effects of  $\text{MnCl}_2$  concentrations on  $\text{MnO}_{2\text{-bio}}$  formation in the absence of BPA for (a) *R. AzwK-3b*, (b) *E. SD-21*, (c) *P. putida* GB-1 at different  $\text{MnCl}_2$  concentrations. Error bars represent the standard deviation of triplicate samples. Error bars smaller than the symbol size are not depicted. .... 21

Figure 2.8 Growth of (a) *R. AzwK-3b*, (b) *E. SD-21*, (c) *P. putida* GB-1 in the presence of different amount of BPA. Error bars represent the standard deviation of triplicate samples. Error bars smaller than the symbol size are not depicted..... 23

Figure 2.9 (a) Relief of growth inhibition for *R. AzwK-3b* with 18  $\mu\text{M}$  BPA in the presence of 100  $\mu\text{M}$   $\text{MnCl}_2$  (b)  $\text{MnO}_{2\text{-bio}}$  formed in the presence of 100  $\mu\text{M}$   $\text{MnCl}_2$  and 18  $\mu\text{M}$  BPA. Error bars represent the standard deviation of triplicate samples. Error bars smaller than the symbol size are not depicted..... 24

Figure 3.1 Cell free  $\text{MnO}_{2\text{-bio}}$  formation (a) Control, (b) cf-C  $\text{MnO}_{2\text{-bio}}$ , (c) cf-P  $\text{MnO}_{2\text{-bio}}$ ..... 31

Figure 3.2 BPA degradation with 0.2 mM cf-C  $\text{MnO}_{2\text{-bio}}$  and cf-P  $\text{MnO}_{2\text{-bio}}$ , (a) without PP at pH 7 (b) with PP at pH 7 (c) without PP at pH 4. Error bars represent the standard deviation of triplicate samples. Error bars smaller than the symbol size are not depicted. .... 35

Figure 3.3 BPA degradation with 0.2 mM MnO<sub>2-syn</sub> (a) without PP at pH 7 (b) with PP at pH 7. Error bars represent the standard deviation of triplicate samples. Error bars smaller than the symbol size are not depicted. .... 36

Figure 3.4 BPA degradation with 0.2 mM MnO<sub>2-syn</sub> free of Mn(III). Error bars represent the standard deviation of triplicate samples. Error bars smaller than the symbol size are not depicted. .... 37

Figure 3.5 An example of a Mn(III)-PP standard curve. .... 38

Figure 3.6 Mn release rate for (a) cf-C MnO<sub>2-bio</sub>, (b) cf-P MnO<sub>2-bio</sub>, (c) hexagonal birnessite and (d) triclinic birnessite. Error bars represent the standard deviation of triplicate samples. Error bars smaller than the symbol size are not depicted. .... 39

Figure 3.7 BPA degradation rates vs Mn(III) content release rates in four MnO<sub>2</sub>. Error bars represent the standard deviation of triplicate samples. .... 40

Figure 3.8 (a) BPA degradation and (b) BPA degradation rates with 0.2 mM synthetic Mn(III) acetate-PP at different PP concentrations (Na-PP). The last legend is for Mn(III) extracted from triclinic birnessite. Error bars represent the standard deviation of triplicate samples. Error bars smaller than the symbol size are not depicted. .... 42

## List of Tables

Table 2.1 BPA degradation rates by MOB at different Mn(II) concentrations. ....	16
Table 2.2 Growth rate constants at different BPA concentrations in the absence of Mn(II) by MOB. .....	22
Table 3.1 BPA degradation rates for synthetic and biogenic MnO <sub>2</sub> .....	34
Table 3.2 Mn(III) content and release rate from different MnO <sub>2</sub> . ....	40
Table 3.3 BPA degradation rates for Mn(III) mediated BPA degradation experiments at different ligand concentration.....	42

## **Acknowledgements**

I would like to express my deepest appreciation and gratitude to my major professor, Dr. Jeongdae Im, who has given me an exciting project to work on. His constant guidance and persistent support have made the journey of my master's study easier and interesting. Surely, the knowledge I have earned from his guidance, will make me a better research professional in the future.

I would like to express my sincere gratitude to Dr. Ganga Hettiarachchi and Dr. Prathap Parameswaran for their kind support as my committee members. Again, I would not be able to finish my research without the help of my husband, Dr. Md Zahidul Karim. I would also like to thank my friends and colleagues Dr. Haripriya Naidu, Niloy Barua, Md Ariful Islam Juel, Kahao Lim, Robert Weil, Maheen Mahmood for their support during my master's journey. I also thank Dr. Ryan Hansen and Dr. Won Min Park from the Department of Chemical Engineering, K-state for giving me access to use equipment from their laboratories and Dr. Madhubhashini Galkaduwa from the Department of Agronomy, K-state for her help in sample analysis for my research.

I would like to acknowledge the collaborators of this project Dr. Frank E. Löffler and Yanchen Sun from University of Tennessee, Knoxville, for their kind support and suggestions towards my research. Finally, I would like to thank the American Chemistry Council for funding this project.

## **Dedication**

To my dearest husband, Zahidul, for constantly being by my side.

## Chapter 1 - Introduction

Bisphenol A (2,2-bis[4-hydroxyphenyl]propane, BPA), a monomer for producing polycarbonate plastic and epoxy resins,<sup>1-3</sup> is one of the most produced chemicals in the world. Chemically, it is a propane with two phenol functional groups (Figure 1.1). BPA was first discovered in 1905, and gradually gained its commercial popularity with time. In 2015, the global demand of BPA was more than 7.7 million tons and is predicted to grow further at a rate of 4.8% yearly, through the year 2022.<sup>4</sup> About 65% of total BPA is used in the production of polycarbonate resins, 28% is used for epoxy resins and the rest is used in manufacturing other products.<sup>5</sup> BPA is used in products of everyday use such as flame retardants, lacquer coatings on food cans, dental sealants, bottle tops and water pipes, and as antioxidants in plastics.<sup>6</sup> It is also used in different products including compact disks, children's toy, thermal papers, electronic equipment, automobiles and so on.<sup>1</sup>

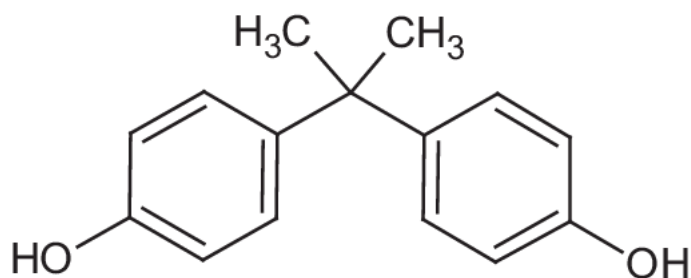


**Figure 1.1 Molecular structure of bisphenol A (BPA).**

Despite its wide ranging usage in consumer products, BPA exposure has been reported to be detrimental to human body as well as to other mammalian and non-mammalian animals.<sup>3</sup> BPA has weak estrogenic properties and it has been identified as an endocrine disrupting compound (EDC).<sup>1</sup> It can bind to an estrogen receptor like natural estrogens and regulate the activity of estrogen responsive genes.<sup>7</sup> Cell function in human body can also be disrupted by estrogenic activity of

BPA.<sup>8</sup> It can also cause reproductive disorder, cardiovascular disease, diabetes and liver disease in human.<sup>9</sup>

Due to its massive production and improper disposal, BPA has entered into the environment. BPA concentrations of 0.5–343  $\mu\text{g kg}^{-1}$  in fresh water sediments,<sup>10,11</sup> 0.5–776  $\text{ng L}^{-1}$  in surface water bodies,<sup>11–13</sup> 0.02–149.2  $\mu\text{g L}^{-1}$  in sewage effluents<sup>14,15</sup> and 1.3–17,200  $\mu\text{g L}^{-1}$  in landfill leachate<sup>16</sup> have been detected in the environment. BPA processing in the manufacture of plastic products, inefficient removal in wastewater treatment, unsupervised leaching of landfill leachate and disintegration of discarded BPA containing materials are the main reasons for the release of BPA into the environment.<sup>12,14,16–19</sup> A recent survey showed that BPA was detected in human urine samples at a frequency of up to 99%.<sup>20</sup> Hence, scientific studies on environmental fate of BPA is of great interest due to health concerns associated with BPA exposure.

BPA can be transferred and degraded by several biotic and abiotic processes upon releasing into the environment. BPA is susceptible to adsorption by suspended solids and sediments, photodegradation, degradation by reactive minerals<sup>1,21</sup> and biodegradation by diverse taxa of bacteria, fungi, algae and plants under oxic conditions.<sup>1,21,22</sup> Known pathways and intermediates in BPA degradation process, mediated by diverse bacteria, fungi, algae and plants as well as reactive mineral phases and are well summarized by Im and Löffler (Figure 1.2).<sup>21</sup>

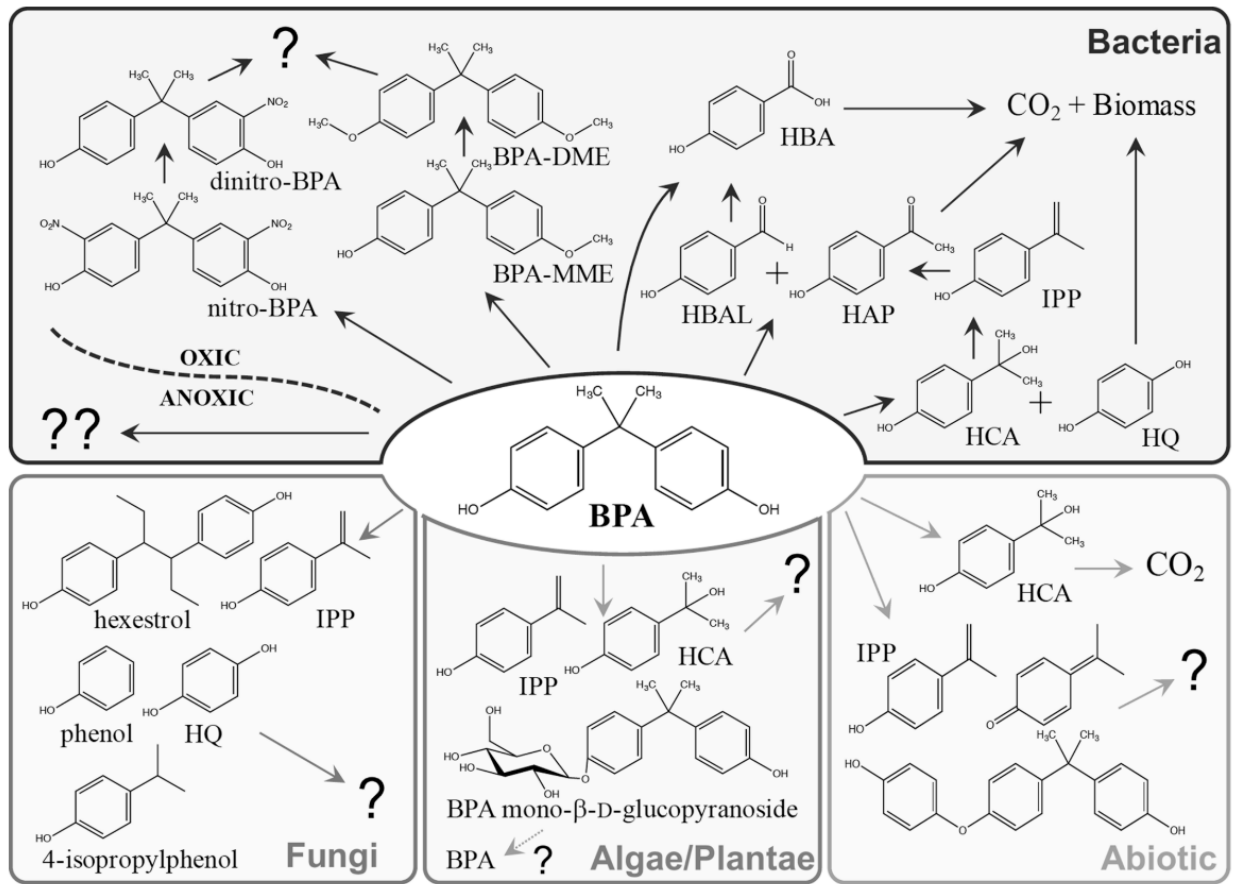


**Figure 1.2 BPA degradation pathways and intermediates mediated by biological entities and reactive mineral phases demonstrated in the laboratory. (Im et al., 2016)**

Under anoxic conditions, on the other hand, many studies concluded that BPA is recalcitrant.<sup>23–26</sup>

However, recently, different studies demonstrated that chemically synthesized manganese oxides ( $\text{MnO}_{2\text{-syn}}$ ) mediate BPA degradation without the requirement of oxygen.<sup>27–33</sup> Manganese oxides ( $\text{MnO}_2$ ) are naturally occurring strong oxidants which are found in subsurface environments, including soils, marine and freshwater sediments.<sup>34</sup> In the BPA degradation by  $\text{MnO}_{2\text{-syn}}$ , hydroxycumyl alcohol (HCA) was detected as a major intermediate with up to 64% of conversion ratio.<sup>30</sup> Nakamura et al. reported that HCA may have higher estrogenic activity than BPA,<sup>35</sup> but HCA is also susceptible to  $\text{MnO}_{2\text{-syn}}$  mediated degradation as well as to microbial degradation

under oxic conditions.<sup>30</sup> MnO<sub>2</sub> are highly reactive and known to affect the fate of metals, nutrients, organic and inorganic compounds<sup>36–39</sup> including various phenolic compounds.<sup>40–43</sup>

The formation of MnO<sub>2</sub> (or biological MnO<sub>2-bio</sub>) is mainly attributed to microbial Mn(II) oxidation.<sup>34,44</sup> Microorganisms that oxidize Mn(II) to MnO<sub>2</sub> are abundant in nature. The oxidation of Mn(II) to MnO<sub>2</sub> or Mn(III/IV) oxides is energetically favorable and microorganisms may harness and utilize energy from these reactions.<sup>34,45,46</sup> However, the physiological function of Mn(II) oxidation has not been established. Bacteria catalyze Mn(II) oxidation by direct and indirect enzymatic reactions.<sup>34</sup> The enzymes responsible for direct Mn(II) oxidation have been identified and studied. Two marine  $\alpha$ -proteobacteria: *Roseobacter* sp. strain AzwK-3b and *Erythrobacter* sp. strain SD-21 and a freshwater  $\gamma$ -proteobacteria: *Pseudomonas putida* strain GB-1 oxidize Mn(II) using different enzymatic activities (Figure 1.3). *R. AzwK-3b* oxidize Mn(II) indirectly through the enzymatic production of extracellular superoxide radicals, named reactive oxygen species (ROS) superoxide.<sup>44</sup> In *E. SD-21*, a Ca<sup>2+</sup> binding heme peroxidase (HPO) enzyme, named MopA (manganese-oxidizing peroxidase) is responsible for Mn(II) oxidation.<sup>47</sup> This enzyme catalyzes Mn(II) oxidation by utilizing Fe-heme to oxidize a substrate and reducing H<sub>2</sub>O<sub>2</sub>.<sup>47</sup> *P. putida* GB-1 employs two multicopper oxidase (MCO) enzymes for Mn(II) oxidation, named MnxG and McoA, and animal heme peroxidase enzyme, MopA.<sup>48</sup> MCOs contain four Cu atoms and catalyzes four electron reduction of O<sub>2</sub> to H<sub>2</sub>O.<sup>49</sup>

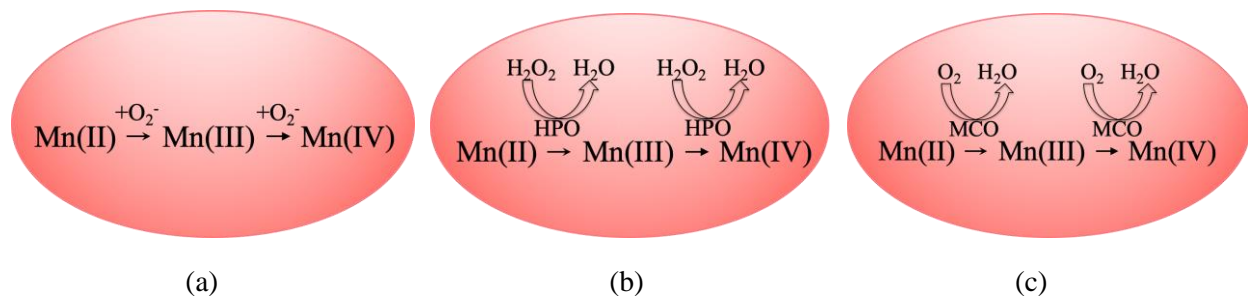


**Figure 1.3 Microbial Mn(II) oxidation with different enzymatic systems in (a) *R. AzwK-3b*, (b) *E. SD-21* and *P. putida* GB-1, (c) *P. putida* GB-1.**

Manganese oxidizing bacteria (MOB) oxidize Mn(II) to MnO<sub>2</sub> by two sequential single-electron transfer reactions where Mn(III) is produced as a transient intermediate.<sup>50-52</sup> In nature, this intermediate Mn(III) can prevail in a soluble ion phase or a solid phase.<sup>50</sup> Mn(III) is very unstable and disproportionates into Mn(II) or Mn(IV) unless complexed by a soluble organic or inorganic chelating agents (Figure 1.4).<sup>53-55</sup> In natural environment, diverse species of microbes have been reported to produce organic ligands which stabilize Mn(III) in aqueous solution. *Erythrobacter* sp. SD-21 produce pyrroloquinoline quinone (PQQ) that stabilizes the Mn(III) intermediate in the oxidation of Mn(II) to Mn(IV).<sup>56</sup> A pyoverdine siderophore produced by the Mn(II)-oxidizing bacterium *Pseudomonas putida* MnB1 also promotes natural Mn(III) chelation by forming Mn(III)-siderophore (Fe-binding ligands) complexes.<sup>55</sup> In laboratory settings, different ligands, such as pyrophosphate, EDTA, and citrate have been used to stabilize Mn(III) by forming Mn(III)-ligand complex.<sup>53,54</sup> Pyrophosphate (PP) is a widely used ligand because it makes strong Mn(III)-PP complex at Mn concentrations and pH values common to aquatic environment.<sup>53</sup> Mn(III)-PP complex can have half-life as low as 5 hours to as high as 500 days corresponding to PP/Mn(III) ratio of 5 to 50.<sup>54</sup>

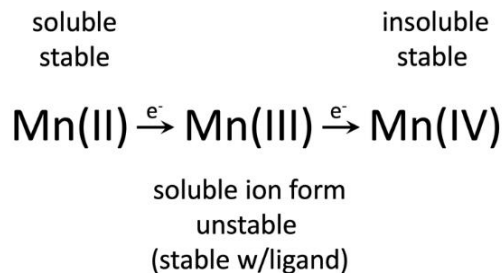


**Figure 1.4 Mn(II) oxidation occurs via two single-electron transfer reactions with Mn(III) as a transient intermediate.**

Mn(III) is also a strong oxidant capable of oxidizing metal, phenols and organic compounds.<sup>57-59</sup>

The reactivity and oxidative properties of Mn(III) can be related to their high redox potential.<sup>60</sup>

Studies have measured Mn(III) content in MnO<sub>2-syn</sub>.<sup>33,61</sup> Huang et al. reported Mn(III) content from 20 to 37% in MnO<sub>2-syn</sub> of different phase structures.<sup>33</sup> Banerjee et al. showed birnessite contain 25% of Mn(III) in their layer vacancy sites.<sup>61</sup> MnO<sub>2</sub> produced by microbial Mn(II) oxidation (MnO<sub>2-bio</sub>) contain Mn(III) in their layered structure.<sup>34,52,62</sup> MnO<sub>2</sub> have been reported to have different reactivity depending on the Mn(III) content.<sup>52</sup> Although it is clear that Mn(III) participates MnO<sub>2</sub>-mediated contaminant transformation, the relative contribution of Mn(III) has not been elucidated.

MnO<sub>2</sub> is a biologically produced reactive mineral that has attracted attention for their roles in degradation of contaminants in the subsurface environments. Therefore, biologically mediated abiotic degradation (BMAD) could emerge as a manageable remediation process.<sup>63,64</sup> This thesis aims at examining BMAD of BPA with three MOB in live culture experiments. The role of Mn(III) in the reactivity of biogenic MnO<sub>2-bio</sub>, produced by one MOB, towards BPA is also examined in this thesis.

## 1.1 Goals and objectives

The primary goal of this thesis is to determine the mechanistic understanding of  $\text{MnO}_{2\text{-bio}}$  mediated BPA degradation. This thesis is combined of two studies. In the first study, BPA degradation in live cultures of three MOB: *R. AzwK-3b*, *E. SD-21* and *P. putida* GB-1 in the presence and absence of Mn(II) is discussed. The objective of this study includes the understanding of the biological components generating mineral phase as well as the mineral phase itself to assess the impact of BMAD process on the fate of BPA in environmental system. The objective of the second study is to evaluate the relative roles of Mn(III) and Mn(IV) in biogenic  $\text{MnO}_{2\text{-bio}}$  produced by the MOB, *R. AzwK-3b*, which is assessed by examining their impacts on BPA degradation under different experimental conditions. In this thesis, chapter 2 and 3 covers study one and two respectively. These two chapters covers detailed information regarding the studies, including the background, materials and methods, results and discussion and the environmental implications of the studies. Chapter 4 includes a brief summary and conclusion of this thesis.

## Chapter 2 - Biologically mediated abiotic degradation (BMAD) of bisphenol A by three Mn(II) oxidizing bacteria

### 2.1 Introduction

Natural MnO<sub>2</sub> is recognized as a strong oxidant and its efficacy to mediate transformation of organic (e.g., antibacterial agents, pesticides, and endocrine disruptors)<sup>38,65</sup> and inorganic contaminants (e.g., HS<sup>-</sup>, heavy metals)<sup>66</sup> have been widely investigated. The formation of MnO<sub>2</sub> mineral phases is not fully understood but attributed to microbial activities. Microorganism catalyze Mn(II) oxidation and produce MnO<sub>2-bio</sub>. Three manganese oxidizing bacteria (MOB) - *Roseobacter* sp. strain AzwK-3B, *Erythrobacter* sp. strain SD-21 and *Pseudomonas putida* strain GB-1 have been extensively studied for their different enzymatic activities catalyzing microbial MnO<sub>2-bio</sub> formation.<sup>34,44,47,67,68</sup> In this study, these MOB are selected to examine the biologically mediated abiotic degradation (BMAD) of BPA by MnO<sub>2-bio</sub> produced by these strains.

Biologically produced reactive mineral phases have attracted attention for their roles in the degradation of priority pollutants in subsurface environments.<sup>64,69</sup> The reactivity of biologically produced MnO<sub>2</sub> (MnO<sub>2-bio</sub>) toward organic contaminants have been demonstrated in live cultures as well as mixed culture reactors amended with Mn(II)<sup>70-72</sup>. In this study, we examined abiotic BPA degradation in cultures of these MOB in the absence and presence of biologically produced MnO<sub>2-bio</sub> with a view to understanding BMAD process. The observations from this study emphasize the relevance of BMAD process in controlling the longevity of BPA in the natural environment.

## 2.2 Materials and methods

### 2.2.1 Chemicals and preparation of $MnO_{2-syn}$

BPA (>99% purity),  $MnCl_2 \cdot 4H_2O$  (>98% purity) and Leucoberbelin blue (LBB, 65% dye content) were purchased from Sigma-Aldrich (St. Louis, MO). Metyrapone [2-methyl-1,2-di-(3-pyridyl)-1-propanone] was purchased from Cayman Chemical Company.  $MnO_{2-syn}$ : Vernadite, was prepared according to established procedures.<sup>106</sup> In brief, Vernadite was synthesized by adding 2.96 g of  $KMnO_4$  in 74.1 mL of distilled water and placed on a hot plate under continuous stirring. When the solution was at 90 °C, 3.71 mL of 5 M NaOH solution was added followed by the addition of 5.55 g of  $MnCl_2$  dissolved in 27.8 mL distilled water slowly.  $MnO_{2-syn}$  particles were collected and washed five times with DI water before storing.  $MnO_{2-syn}$  was stored in liquid suspension which has a nominal concentration of 0.4 M.

### 2.2.2 BPA degradation by MOB with varying concentrations of Mn(II)

*R. AzwK-3b* and *E. SD-21* were maintained in an organic-rich K medium (2 g L<sup>-1</sup> peptone, 0.5 g L<sup>-1</sup> yeast extract, 20 mM HEPES buffer, pH 7.5) prepared with 75% (vol/vol) artificial seawater (K-ASW).<sup>44</sup> *P. putida* GB-1 was grown in Lept media (0.5 g/L yeast extract, 0.5 g/L casamino acids, 5 mM glucose, 0.48 mM calcium chloride, 0.83 mM magnesium sulfate, 3.7 μM iron (III) chloride, trace metal solution containing: 0.04 μM copper sulfate, 0.15 μM zinc sulfate, 0.08 μM cobalt chloride, 0.06 μM sodium molybdate and 10 mM HEPES buffer pH 7.5).<sup>73</sup> BPA was added in the mediums before sterilization, as it is not readily soluble at room temperature. Mn(II) was added from a 100 mM  $MnCl_2$  sterile stock solution aseptically. Culture vessels containing 100 ml medium in 250 mL Erlenmeyer flasks capped with aluminum foil were incubated at 30 °C and on

a shaker (120 rpm) in the dark. Un-inoculated (sterile) cultures were prepared as negative controls. All the experiments were done in triplicates.

BPA degradation experiment without Mn(II) was conducted with *R. AzwK-3b* in a defined medium, J acetate medium (10 mM sodium acetate, 10 ml L<sup>-1</sup> vitamin mix (in mg L<sup>-1</sup>: biotin, 320; niacin, 32; thiamin, 16; 4- aminobenzoic acid, 32; calcium pantothenic acid, 16; pyridoxine, 160; vitamin B12, 16; riboflavin, 32; folic acid, 32), 1 ml L<sup>-1</sup> 8% NH<sub>4</sub>Cl, 2 mM KHCO<sub>3</sub>, 0.2 ml L<sup>-1</sup> 10% KH<sub>2</sub>PO<sub>4</sub>, and 3.6 μM iron (as FeSO<sub>4</sub>.7H<sub>2</sub>O) complexed to 78 μM nitrilotriacetic acid, buffered to pH 7.6 with 20 mM HEPES, and prepared as 50% (volume) artificial seawater).<sup>74</sup> Here acetate was used as the sole carbon source and BPA concentration was 9 μM. *E. SD-21* was grown in K medium with 20 μM BPA in the presence and absence of 5mM metyrapone, which is an inhibitor to the enzyme cytochrome P450.<sup>75</sup>

The inhibitory effect of BPA on the growth of *R. AzwK-3b* was assessed with 0, 9, 18 and 44 μM BPA and on the growths of *E. SD-21* and *P. putida* GB-1 with 0, 18 and 44 μM BPA in the absence of Mn(II). The effect of different concentrations of Mn(II) on BPA degradation and MnO<sub>2</sub>-bio formation by *R. AzwK-3b*, *E. SD-21* and *P. putida* GB-1 was examined by adding 9, 18 and 18 μM of BPA (non-inhibitory concentration) respectively amended with 0, 10, 100, and 500 μM of Mn(II). The effect of different concentrations (0, 10, 100, and 500 μM ) of Mn(II) on MnO<sub>2</sub>-bio formation by the three MOB without BPA was also observed. BPA was measured using HPLC analysis and MnO<sub>2</sub>-bio was measured using colorimetric LBB assay.<sup>76</sup>

### ***2.2.3 Abiotic BPA degradation by MnO<sub>2</sub>-syn with and without Mn(II)***

Abiotic BPA degradation experiment in the presence and absence of 500 μM Mn(II) using MnO<sub>2</sub>-syn was conducted. Experiment was conducted in 160 mL glass serum bottles in a total volume of

100 mL having a BPA concentration of 44  $\mu\text{M}$  with and without 500  $\mu\text{M}$  Mn(II) buffered with 5 mM phosphate at pH 7. The reaction was initiated by mixing  $\text{MnO}_{2\text{-syn}}$  from stock solution to achieve a concentration of 2 mM. Aliquots (0.5 mL) of the reaction mixture were collected periodically and transferred to 2 mL glass HPLC vials containing 20  $\mu\text{L}$  of L-ascorbic acid solution (50 mg  $\text{mL}^{-1}$ ) and immediately vortexed for 5 sec. Ascorbic acid quenches the reaction by converting any remaining  $\text{MnO}_{2\text{-syn}}$  to soluble Mn(II) and liberates any sorbed BPA and reaction products.<sup>30</sup> The experiment was conducted in triplicates.

#### ***2.2.4 Analytical procedures***

Due to the hydrophobic nature of BPA (log  $K_{\text{ow}}$  of 2.2 – 3.82),<sup>1</sup> adsorption of BPA onto hydrophobic cell surface components has been reported by several studies<sup>77,78</sup> but a validated methanol extraction procedure confirmed that the adsorption is negligible at the highest  $\text{OD}_{600}$  value observed in this study for each culture.<sup>78</sup> Therefore, for the quantification of BPA and HCA in live cultures, 1 mL of the samples were centrifuged for 10 minutes at 13,200 rpm to pellet solids, and then the supernatant was subjected to HPLC analysis. An Agilent 1100 Series HPLC system equipped with a diode array detector (DAD) and a fluorescence detector (FLD) in series was used. A reverse-phase Agilent Eclipse XDB C18 column (4.6 mm  $\times$  150 mm, 5  $\mu\text{m}$ ) was used for isocratic separation with an acetonitrile-water (50:50, v/v) eluent at a flow rate of 1  $\text{mL min}^{-1}$ .<sup>30</sup> The conversion efficiency of BPA to HCA was calculated on a molar basis, by dividing the amount ( $\mu\text{mol}$ ) HCA formed by the amount BPA degraded ( $\mu\text{mol}$ ) over time.  $\text{MnO}_2$  was quantified using a colorimetric LBB assay as previously described<sup>76</sup> using flat bottom 96 well plate. For standard curve preparation, 30  $\mu\text{L}$  of  $\text{KMnO}_4$  dilutions spanning a concentration range from 7 to 100  $\mu\text{M}$  were aliquoted into empty wells followed by the addition of 270  $\mu\text{L}$  LBB solution (40 mg LBB in 100 mL 45 mM acetic acid). For synthetic  $\text{MnO}_{2\text{-syn}}$ , samples were diluted and mixed with LBB

solution at a ratio of 1:10. For  $\text{MnO}_{2\text{-bio}}$  quantification in live cultures, 50  $\mu\text{L}$  samples were collected in 2 ml centrifuge tubes and mixed with 450  $\mu\text{L}$  LBB solution. All samples were incubated at room temperature for 15 minutes in the dark, centrifuged for 1 minute at 13200 rpm to pellet solids, and 300  $\mu\text{L}$  of the supernatant was transferred to the 96-well plate. Absorbance was measured at 618 nm using a plate reader, Epoch 2 microplate spectrophotometer (BioTek Instruments, Inc., Winooski, VT, USA). Growth of the strains were monitored by measuring absorbance of live cultures at 600 nm using the same instrument. 12  $\mu\text{L}$  L-ascorbic acid solution (50 mg  $\text{mL}^{-1}$ ) was added to individual wells prior to growth measurement, to dissolve  $\text{MnO}_{2\text{-bio}}$  and prevent interferences.

## 2.3 Results

### 2.3.1 BPA degradation by MOB without Mn(II)

When the three MOB were incubated with BPA in the absence of Mn(II), degradation occurred (Figure 2.1 a, c, e). For *R. AzwK-3b* and *E. SD-21*, 30% and 87% BPA was degraded in 3 days at a rate of  $0.12 \pm 0.04 \text{ day}^{-1}$  and  $0.62 \pm 0.28 \text{ day}^{-1}$  (Table 2.1; Figure 2.1 a, c) respectively in the absence of Mn(II). For *R. AzwK-3b*, BPA degradation ceased in late stationary phase, suggesting that the degradation may be fortuitous. *E. SD-21* degraded BPA completely in 4 days. *P. putida* GB-1 degraded only 10% of BPA over a time of 2 days at a rate of  $0.05 \pm 0.03 \text{ day}^{-1}$  without Mn(II) (Table 2.1; Figure 2.1 e).

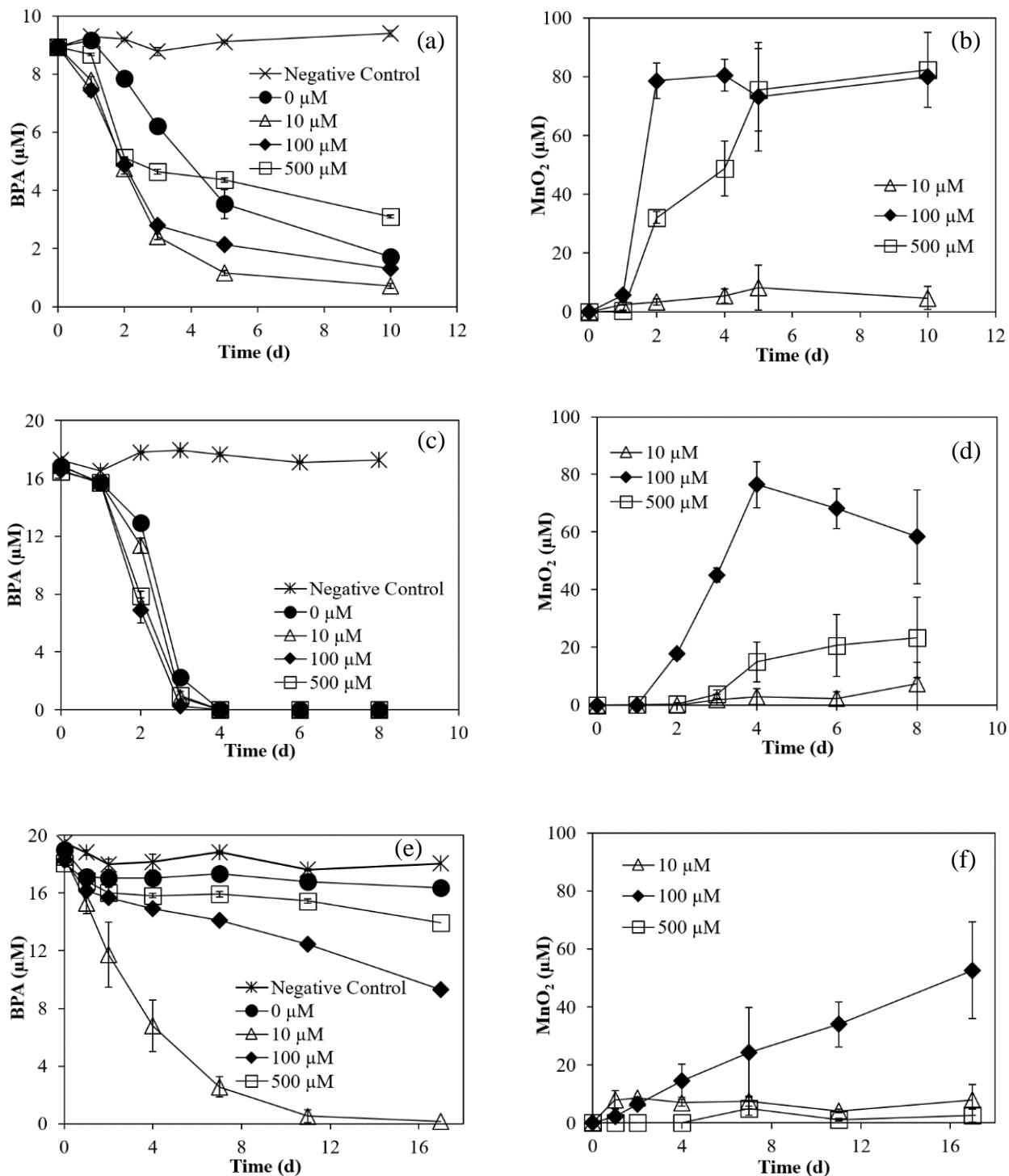


**Figure 2.1** BPA degradation (left column) and  $\text{MnO}_2$ -bio formation (right column) at different  $\text{MnCl}_2$  concentration for (a), (b) *R. AzwK-3b*, (c), (d) *E. SD-21* and (e), (f) *P. putida* GB-1. Error bars represent the standard deviation of triplicate samples. Error bars smaller than the symbol size are not depicted.

To see if MOB can utilize BPA as source of energy, *R. AzwK-3b* and *E. SD-21* were inoculated in mineral salt medium (separately) in the presence of BPA as a sole carbon source, but both of them did not grow (data not shown). However, *R. AzwK-3b* grew in J acetate medium<sup>74</sup> amended with 9  $\mu\text{M}$  BPA without Mn(II) and showed BPA degradation when incubated with BPA (Figure 2.2).

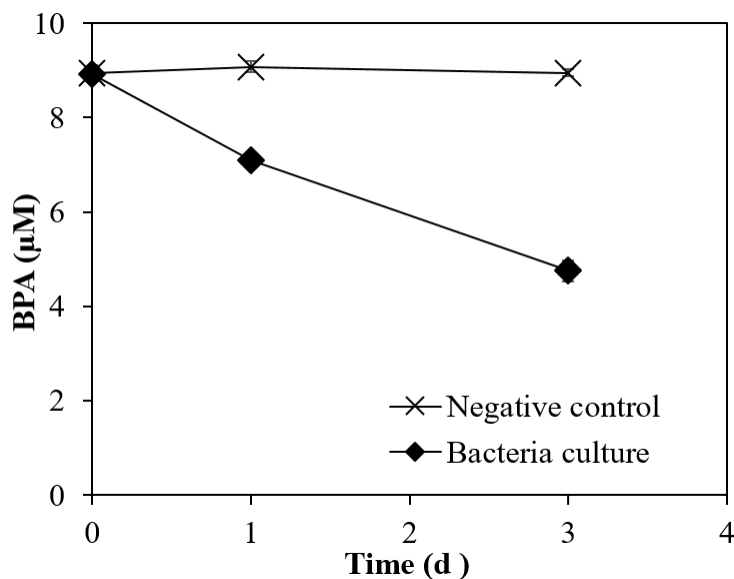


**Figure 2.2 BPA degradation without Mn(II) in J acetate medium with *R. AzwK-3b*. Error bars represent the standard deviation of triplicate samples. Error bars smaller than the symbol size are not depicted.**

To examine if the inhibitor metyrapone affects the BPA transformation catalyzing enzyme cytochrome P450, *E. SD-21* was incubated with 20  $\mu\text{M}$  BPA in K medium in the presence and absence of 5mM metyrapone. However, BPA degradation showed similar trend in the presence and absence of the inhibitor (Figure 2.3).

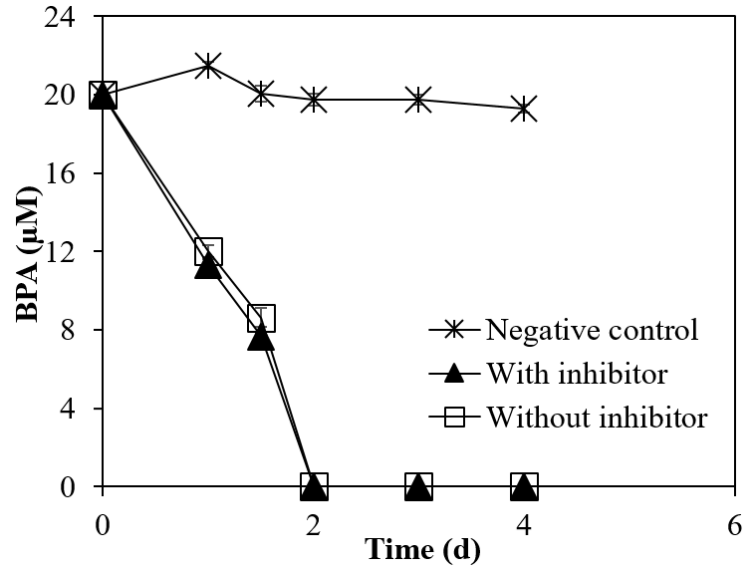


**Figure 2.3 BPA degradation in the presence and absence of inhibitor metyrapone with *E. SD-21*. Error bars represent the standard deviation of triplicate samples. Error bars smaller than the symbol size are not depicted.**

### 2.3.2 BPA degradation by *MOB* with *Mn(II)*

For all three strains, BPA degradation was significantly enhanced in the presence of *Mn(II)* (Figure 2.1 a, c, e). The *Mn(II)* concentration that induced the highest BPA degradation rate was different among different strains. For *R. AzwK-3b* and *P. putida* GB-1, highest BPA degradation rates ( $0.44 \pm 0.09$  and  $0.23 \pm 0.02 \text{ day}^{-1}$  respectively) were observed with  $10 \mu\text{M}$  *Mn(II)* even though  $\text{MnO}_{2\text{-bio}}$  produced was not high (Figure 2.1 a, b, e, f; Table 2.1). For *E. SD-21*, highest BPA degradation ( $1.33 \pm 0.52 \text{ day}^{-1}$ ) was observed with  $100 \mu\text{M}$  *Mn(II)* (Figure 2.1 c; Table 2.1). BPA degradation rates vs  $\text{MnO}_{2\text{-bio}}$  formation was plotted for different *Mn(II)* concentration for all three *MOB* (Figure 2.4). With increasing *Mn(II)* concentrations, BPA degradation rates decreased. For *R. AzwK-3b* and *P. putida* GB-1,  $100 \mu\text{M}$  *Mn(II)* amended cultures produced higher  $\text{MnO}_{2\text{-bio}}$  ( $80$  and  $52 \mu\text{M}$ ) but BPA degradation rates ( $0.39 \pm 0.1$  and  $0.08 \pm 0.03 \text{ day}^{-1}$  respectively) were not higher (Figure 2.1 a, b, e, f; Figure 2.4 a, c; Table 2.1). In vessels amended with  $500 \mu\text{M}$   $\text{MnCl}_2$ , about  $82$  and  $23 \mu\text{M}$   $\text{MnO}_{2\text{-bio}}$  was formed with the strains *R. AzwK-3b* and *E. SD-21* respectively

but only 2.5  $\mu\text{M}$   $\text{MnO}_{2\text{-bio}}$  was formed with *P. putida* GB-1 (Figure 2.1 b, d, f). Therefore, BPA degradation rates did not correlate with  $\text{MnO}_{2\text{-bio}}$  amounts observed in the cultures (Figure 2.4). To examine the blockage of  $\text{MnO}_2$  by excess Mn(II),  $\text{MnO}_{2\text{-syn}}$  mediated BPA degradation experiment was conducted with and without 500  $\mu\text{M}$   $\text{MnCl}_2$ .  $\text{MnO}_{2\text{-syn}}$  in the presence of  $\text{MnCl}_2$  did not show any BPA degradation but in the absence of  $\text{MnCl}_2$ , BPA was degraded at a rate of  $0.042 \pm 0.002 \text{ min}^{-1}$  (Figure 2.5).

HCA, which has been observed as a major BPA degradation intermediate,<sup>30</sup> was detected under all incubation condition with all three strains at all  $\text{MnCl}_2$  concentrations tested (Figure 2.6). The identity of HCA was confirmed by the peak in the HPLC at a retention time 1.7 min. BPA to HCA conversion was also calculated which is shown for all three bacteria (Figure 2.6).

**Table 2.1 BPA degradation rates by MOB at different Mn(II) concentrations.**

Strain	BPA degradation rates, k ( $\text{d}^{-1}$ )			
	k <sub>0 <math>\mu\text{M}</math></sub> <sup>a</sup>	k <sub>10 <math>\mu\text{M}</math></sub>	k <sub>100 <math>\mu\text{M}</math></sub>	k <sub>500 <math>\mu\text{M}</math></sub>
<i>Roseobacter</i> sp. strain AzwK-3b	$0.12 \pm 0.04$	$0.44 \pm 0.09$	$0.39 \pm 0.1$	$0.25 \pm 0.06$
<i>Erythrobacter</i> sp. strain SD-21	$0.62 \pm 0.28$	$0.92 \pm 0.42$	$1.33 \pm 0.42$	$0.91 \pm 0.33$
<i>Pseudomonas putida</i> strain GB-1	$0.05 \pm 0.03$	$0.23 \pm 0.02$	$0.08 \pm 0.03$	$0.06 \pm 0.006$

a Subscript of k represents different  $\text{MnCl}_2$  concentrations.

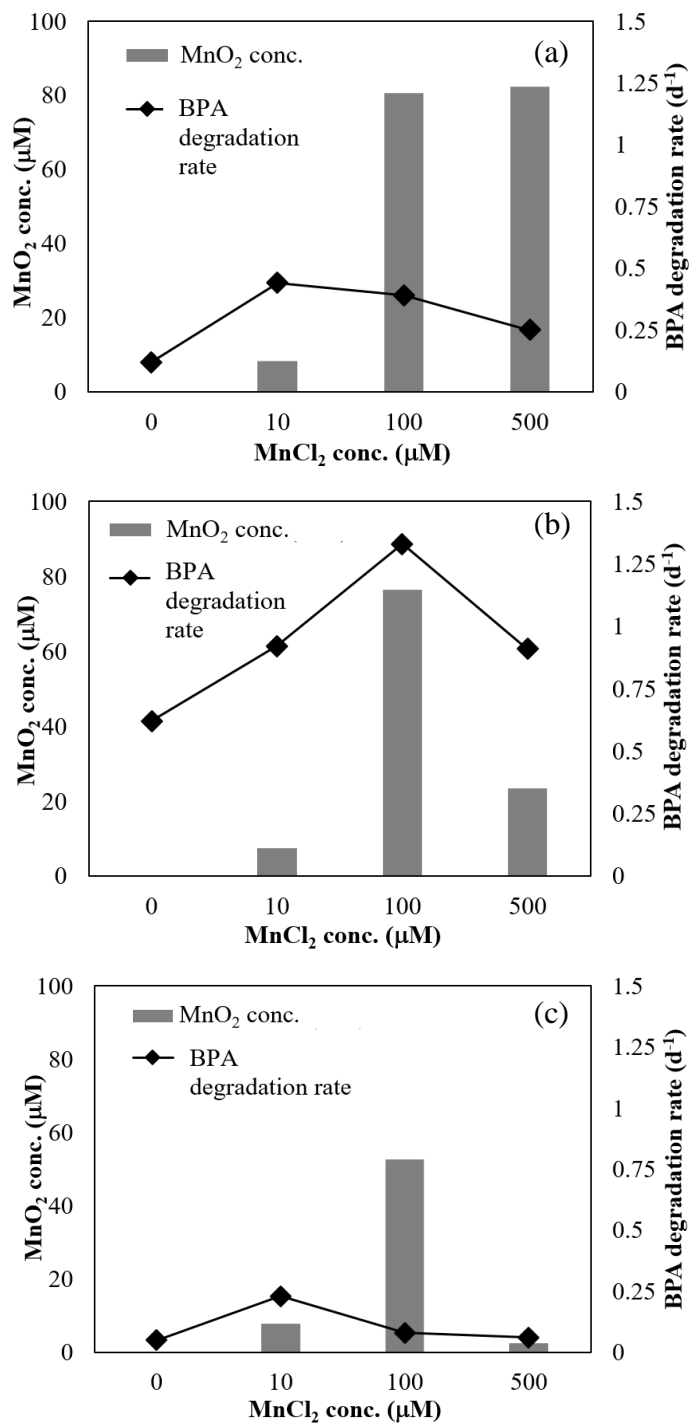


**Figure 2.4 BPA degradation vs MnO<sub>2</sub> formation at different MnCl<sub>2</sub> concentration for (a) *R. AzwK-3b*, (b) *E. SD-21* and (d) *P. putida* GB-1. Error bars represent the standard deviation of triplicate samples. Error bars smaller than the symbol size are not depicted.**

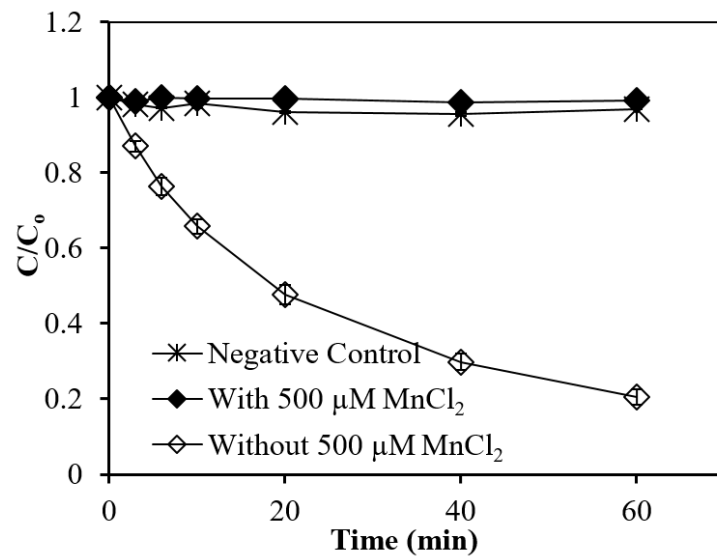


**Figure 2.5 BPA degradation in the presence and absence of 500 μM MnCl<sub>2</sub> in solutions containing 44 μM BPA and 2 mM MnO<sub>2-syn</sub>. Error bars represent the standard deviation of triplicate samples. Error bars smaller than the symbol size are not depicted.**

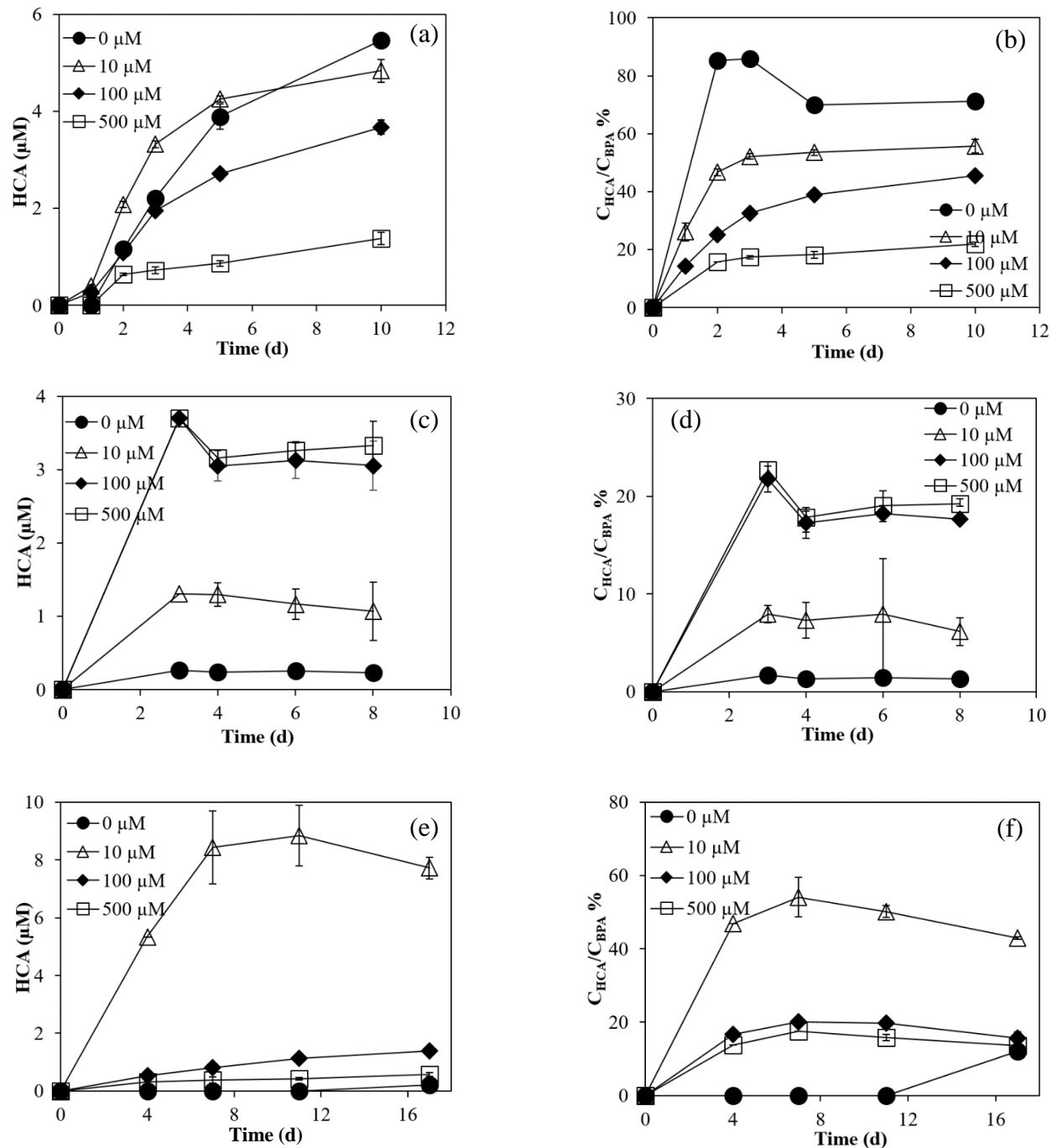


**Figure 2.6 HCA formation (left column) and conversion ratio from BPA to HCA (right column) for (a), (b) *R. AzwK-3b*, (c), (d) *E. SD-21* and (e), (f) *P. putida* GB-1 at different  $\text{MnCl}_2$  concentrations. Error bars represent the standard deviation of triplicate samples. Error bars smaller than the symbol size are not depicted.**

### ***2.3.3 MnO<sub>2-bio</sub> formation in MOB in the absence of BPA***

MnO<sub>2-bio</sub> formation did not correspond to MnCl<sub>2</sub> added for all three cultures in the absence of BPA (Figure 2.7). For *R. AzwK-3b*, higher MnO<sub>2-bio</sub> formation was observed with higher MnCl<sub>2</sub>. With 10, 100, 500 μM MnCl<sub>2</sub>, nominal MnO<sub>2-bio</sub> concentration of 5, 89 and 96 μM was observed after 5 days for *R. AzwK-3b* (Figure 2.7 a). For *E. SD-21*, highest MnO<sub>2-bio</sub> formation for 10 and 100 μM MnCl<sub>2</sub> was 2.35 and 51 μM respectively. However, for 500 μM MnCl<sub>2</sub>, MnO<sub>2-bio</sub> formation was rather repressed showing 9 μM of nominal concentration (Figure 2.7 b). In the case of *P. putida* GB-1, MnO<sub>2-bio</sub> formation for 10 and 100 μM MnCl<sub>2</sub> was positively correlated (7 and 78 μM respectively) but lower amount of MnO<sub>2-bio</sub> (1.4 μM) was formed in the incubation with 500 μM MnCl<sub>2</sub> (Figure 2.7 c)

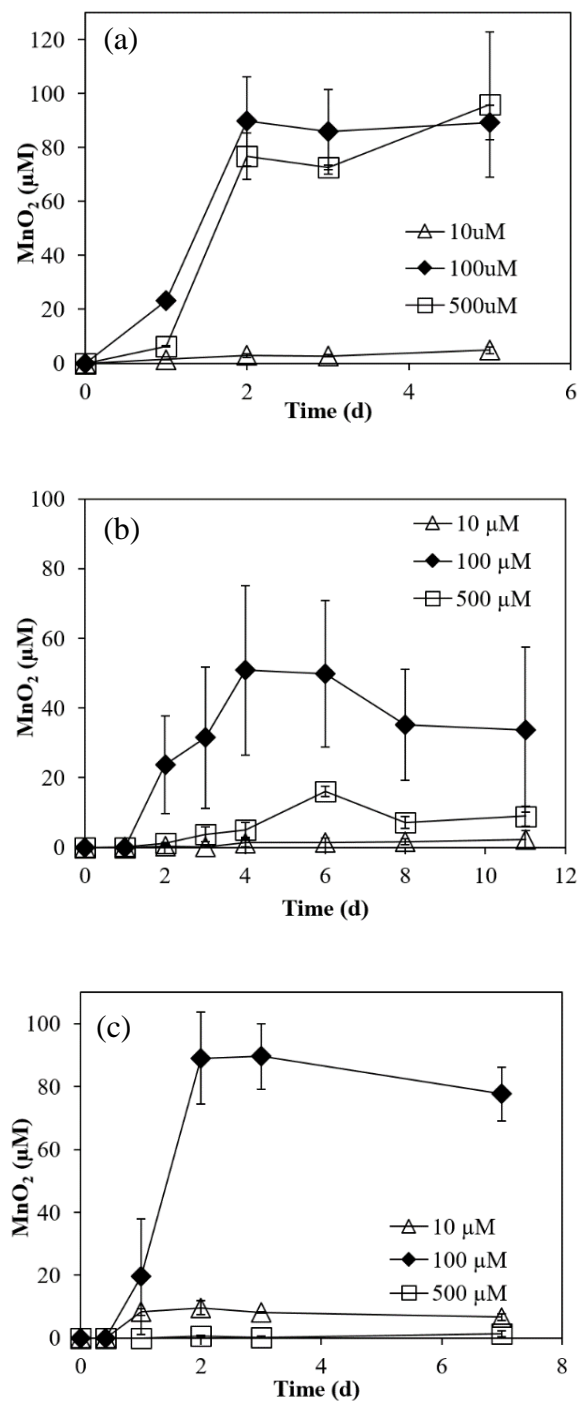


**Figure 2.7** Effects of  $MnCl_2$  concentrations on  $MnO_{2-bio}$  formation in the absence of BPA for (a) *R. AzwK-3b*, (b) *E. SD-21*, (c) *P. putida* GB-1 at different  $MnCl_2$  concentrations. Error bars represent the standard deviation of triplicate samples. Error bars smaller than the symbol size are not depicted.

### 2.3.4 Effect of BPA on the growth of MOB

Higher BPA concentration can inhibit the growth of the bacteria culture in the absence of Mn(II). In the absence of BPA, growth rate of *R. AzwK-3b*, *E. SD-21* and *P. putida* GB-1 was  $1.44 \pm 0.84$  day<sup>-1</sup>,  $2.26 \pm 0.47$  day<sup>-1</sup> and  $5.96 \pm 3.14$  day<sup>-1</sup> respectively (Figure 2.8, Table 2.2). For *R. AzwK-3b*, BPA concentration of 18  $\mu$ M and above showed significant growth inhibition (Figure 2.8 a). Also, the maximum growth yield decreased by 40% in the presence of 44  $\mu$ M BPA. The addition of 100  $\mu$ M MnCl<sub>2</sub> relieved the inhibitory effect of BPA on *R. AzwK-3b* for a BPA concentration of 18  $\mu$ M by forming MnO<sub>2-bio</sub> (Figure 2.9 a, b). For *E. SD-21* and *P. putida* GB-1, growth inhibition was not apparent with BPA concentration up to 44  $\mu$ M (Figure 2.8 b, c).

**Table 2.2 Growth rate constants at different BPA concentrations in the absence of Mn(II) by MOB.**

Strain	Growth rate (d <sup>-1</sup> )			
	For 0 $\mu$ M	For 9 $\mu$ M	For 18 $\mu$ M	For 44 $\mu$ M
<i>Roseobacter</i> sp. strain AzwK-3B	$1.44 \pm 0.84$	$1.57 \pm 0.5$	$1.34 \pm 0.27$	$0.642 \pm 0.09$
<i>Erythrobacter</i> sp. strain SD-21	$2.26 \pm 0.47$	x	$2.16 \pm 0.38$	$1.84 \pm 0.25$
<i>Pseudomonas putida</i> strain GB-1	$5.96 \pm 3.14$	x	$5.62 \pm 2.97$	$5.3 \pm 2.66$

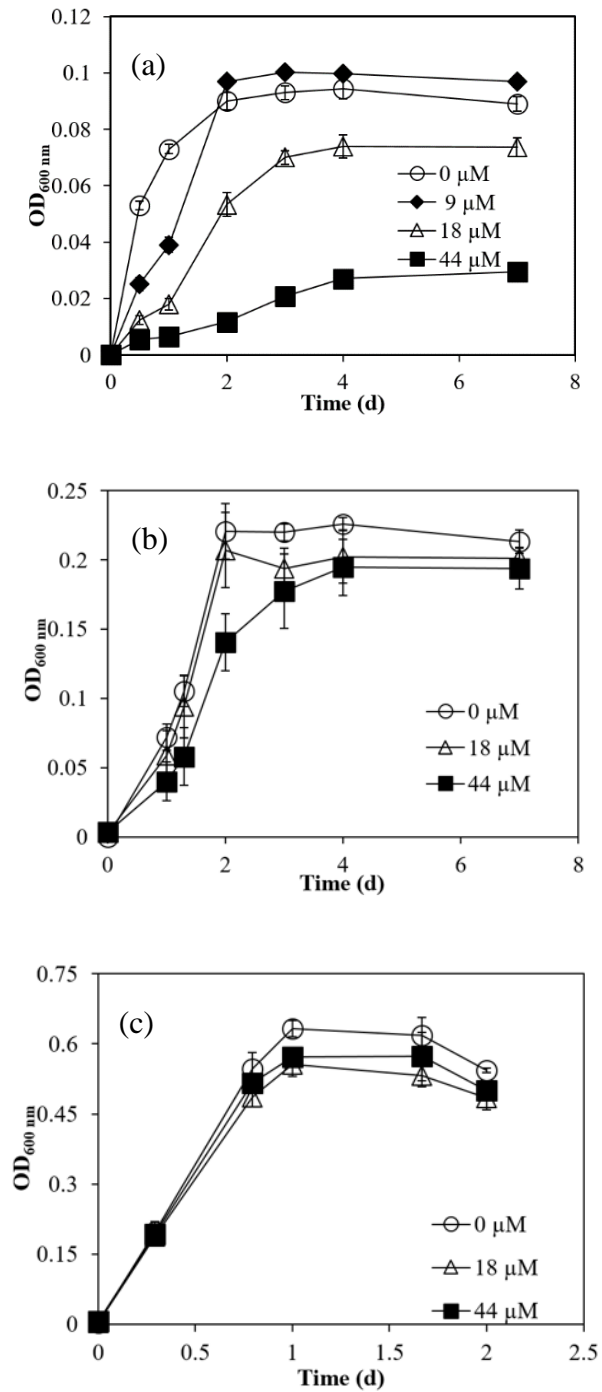


**Figure 2.8 Growth of (a) *R. AzwK-3b*, (b) *E. SD-21*, (c) *P. putida* GB-1 in the presence of different amount of BPA. Error bars represent the standard deviation of triplicate samples. Error bars smaller than the symbol size are not depicted.**

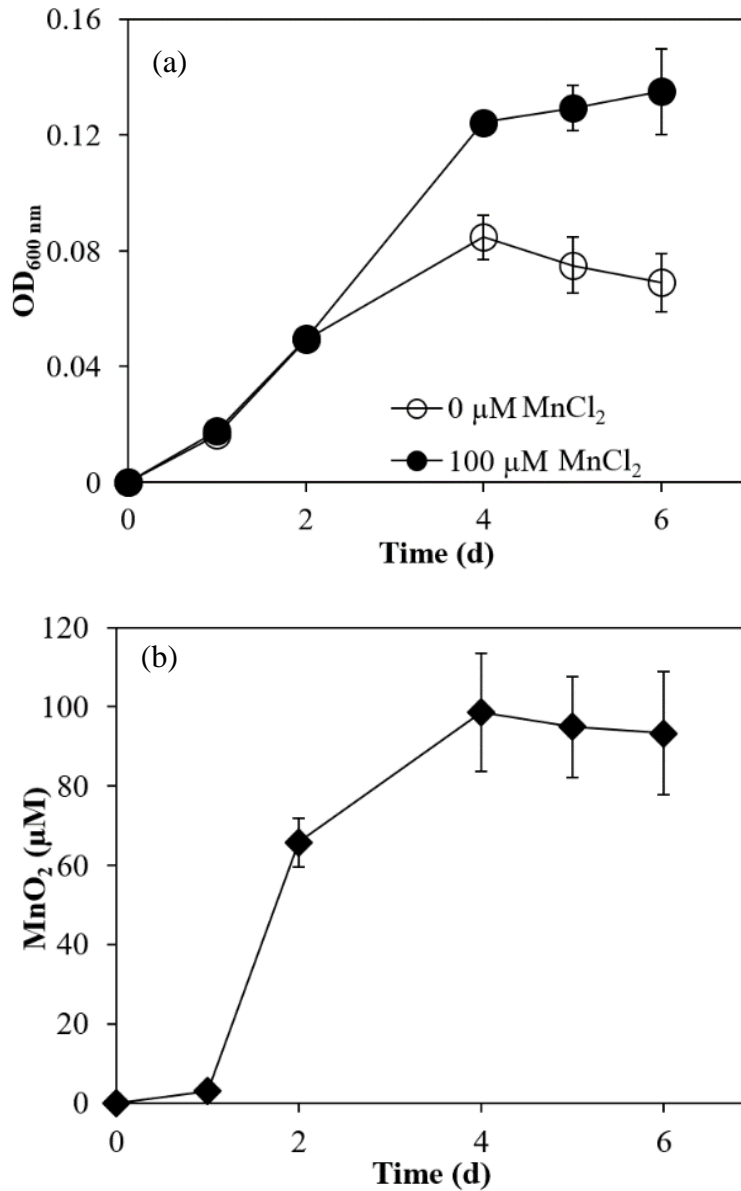


**Figure 2.9 (a) Relief of growth inhibition for *R. AzwK-3b* with 18 μM BPA in the presence of 100 μM MnCl<sub>2</sub> (b) MnO<sub>2</sub>-bio formed in the presence of 100 μM MnCl<sub>2</sub> and 18 μM BPA. Error bars represent the standard deviation of triplicate samples. Error bars smaller than the symbol size are not depicted.**

## 2.4 Discussion

MnO<sub>2</sub> is an oxidizing compound that plays an important role in oxidative degradation of many organic and inorganic compounds and metals.<sup>79</sup> Microorganisms including bacteria and fungi, are known to catalyze Mn(II) oxidation leading to MnO<sub>2</sub> formation in natural and engineered environments. Mn(II)-oxidizing microorganisms discussed in this study are phylogenetically diverse<sup>80</sup> but their Mn(II) oxidation process has some common traits: Mn(II) oxidation follows enzymatic activity, MnO<sub>2</sub> formed are nanoparticulate, birnessite type minerals<sup>52,74,81</sup> and Mn(II) oxidation to MnO<sub>2</sub> consists of two sequential single-electron-transfer reactions. MnO<sub>2</sub> formation occurred at different growth phases in these MOB. *R. AzwK-3b* oxidized Mn(II) in the mid-exponential phase.<sup>82</sup> In the culture vessels incubated with *R. AzwK-3b*, within 1 day, MnO<sub>2</sub> formation was visually apparent due to a golden color and the MnO<sub>2</sub> concentration was less. After 2 to 3 days, discrete brown MnO<sub>2</sub> particles were formed with a higher MnO<sub>2</sub> concentration (Figure 2.1 b; Figure 2.7 a). *E. SD-21* and *P. putida* GB-1 oxidized Mn(II) in their early stationary phase<sup>68,83</sup> which is believed to form as a result of starvation.<sup>68</sup> This caused apparent MnO<sub>2</sub> formation after 2 days (Figure 2.1 d,f; Figure 2.7 b, c).

The experiments with all three MOB demonstrated that increasing MnCl<sub>2</sub> concentrations impeded BPA degradation. For *R. AzwK-3b* and *P. putida* GB-1, BPA degradation was highest with 10 μM MnCl<sub>2</sub> (Figure 2.1 and 2.4) whereas for *E. SD-21*, 100 μM Mn(II) induced fastest BPA degradation (Figure 2.1). BPA degradation was slower for the higher MnCl<sub>2</sub> concentration for all three strains although more MnO<sub>2-bio</sub> formed at relatively higher MnCl<sub>2</sub> concentration (Figure 2.1 and 2.4). A plausible explanation is that the sorption of excess Mn(II) to MnO<sub>2-bio</sub> impacted their reactivity. MnO<sub>2-syn</sub> in the presence of metal ions, particularly excess Mn(II) has been reported to suppress BPA degradation.<sup>27</sup> This was further demonstrated with abiotic BPA degradation experiment with

MnO<sub>2-syn</sub> in the presence and absence of the 500 μM MnCl<sub>2</sub> (Figure 2.5), which was used as the highest MnCl<sub>2</sub> concentration in the live cultures.

One of the attractive features of MnO<sub>2</sub> as an effective scavenger of environmental contaminants is the ability of Mn-oxidizing bacteria to regenerate the reactive oxides.<sup>34,38</sup> High BPA degradation rate occurred with 10 μM MnCl<sub>2</sub> in all three MOB (Figure 2.1 and 2.4). This suggests, MnO<sub>2-bio</sub> was regenerated in the cultures with 10 μM MnCl<sub>2</sub> which continuously degraded BPA. Microbial Mn(II) oxidation coupled with abiotic Mn(IV) reduction, i.e., contaminants transformation, constitutes an efficient cycle, and a small amount of Mn can potentially turnover a substantial amount of BPA. In other words, Mn flux is a relevant metric that has not been considered in many laboratory studies, but is obviously important to gauge the MnO<sub>2-bio</sub>-mediated degradation activity, particularly when the data are used to extrapolate to environmental conditions.

In this study, *R. AzwK-3b* and *E. SD-21* showed BPA degradation in the absence of MnCl<sub>2</sub> (Figure 2.1 a, c). K medium being a rich medium has trace amount (0.3 μM calculated by ICP-MS) of Mn in it which was thought to induce BPA degradation in the absence of Mn(II) for these two strains. However, when *R. AzwK-3b* was grown in Mn free J acetate medium<sup>74</sup>, BPA was degraded (Figure 2.2). Therefore, the BPA degradation by different MnCl<sub>2</sub> for *R. AzwK-3b* is due to the combined effect of both the culture and the MnO<sub>2-bio</sub>. To date, diverse bacterial species belonging to the α-proteobacteria, β-proteobacteria, γ-proteobacteria, bacillus, and actinobacteria have demonstrated BPA degradation.<sup>21</sup> The enzyme cytochrome P450 catalyzed BPA degradation in many bacterial strains<sup>21</sup> and this enzyme was found in *E. SD-21* when searched in the NCBI database.<sup>107</sup> Cytochrome P450 can be inhibited by a chemical, metyrapone.<sup>84</sup> BPA degradation experiment in live cultures of *E. SD-21* with and without metyrapone showed similar BPA degradation trend suggesting no involvement of cytochrome P450 in BPA degradation within this strain (Figure 2.3).

Studies have shown that HCA is the major BPA transformation product in incubations with  $\text{MnO}_2$ .<sup>30,31</sup> HCA was also proposed as a hypothetical BPA transformation product in aerobic bacterial degradation.<sup>75,85</sup> In this study, all three MOB showed the formation of HCA in the incubation system. The concentration of HCA was corresponding with BPA degradation rates (Figure 2.6). Conversion ratio of BPA to HCA was not the same for all the incubation system as observed in a previous study for BPA degradation with  $\text{MnO}_{2\text{-syn}}$ <sup>30</sup> (Figure 2.6). This may be due to the combined effect of both the culture and the  $\text{MnO}_{2\text{-bio}}$  on BPA degradation.

BPA concentrations at 18  $\mu\text{M}$  and above inhibited growth of *R. AzwK-3b* (Figure 2.8 a). This growth inhibition was relieved when  $\text{MnO}_{2\text{-bio}}$  was formed after the addition of 100  $\mu\text{M}$   $\text{MnCl}_2$  (Figure 2.9). It is possible that  $\text{MnO}_{2\text{-bio}}$  formation is a cellular defense for *R. AzwK-3b* in response to evade growth inhibition. Indeed, Mn(II) oxidation and  $\text{MnO}_{2\text{-bio}}$  formation have been proposed to protect bacteria cells from toxic metals and reactive oxygen species.<sup>34,86</sup> For *E. SD-21* and *P. putida* GB-1, growth was not affected by higher BPA concentration suggesting that their enzymatic activities relative to growth may be independent of external BPA concentrations.

The experiments used optimized medium and incubation conditions for all three MOB. The limitations for microbial Mn(II) oxidation under in situ conditions are unclear but effects of carbon source<sup>87</sup> and/or other nutrient availability<sup>71</sup> has been demonstrated. Further research is needed to delineate conditions that affect microbial Mn(II) oxidation activity so that the contribution of  $\text{MnO}_{2\text{-bio}}$  for in situ BPA degradation can be estimated. BPA has been detected in ecosystems at concentrations reaching 1  $\mu\text{M}$  in seawater, 8.5  $\mu\text{g kg}_{\text{-dw}}^{-1}$  in coastal sediment and 0.5–343  $\mu\text{g kg}^{-1}$  in fresh water sediments.<sup>10,21,88</sup> Members of these bacteria are abundant in various marine and freshwater environments which play significant roles in the global carbon and sulfur cycles.<sup>89,90</sup> Therefore, the interplay between BPA and Mn(II)-oxidizing microorganisms in the ecosystem

should be further investigated not only in terms of BPA degradation by  $\text{MnO}_{2\text{-bio}}$ , but also to evaluate possible BPA impacts on organisms involved in biogeochemical cycling.

## **2.5 Environmental implications**

BPA has been detected in anoxic sediments, but many studies concluded that BPA is recalcitrant to microbial degradation under anoxic conditions.<sup>24,26,91</sup> The incubation of BPA with the Mn(II) oxidizing bacteria in the presence of  $\text{MnCl}_2$  demonstrated that (i) lower amount of  $\text{MnO}_{2\text{-bio}}$  effectively degraded BPA, and (ii) Mn flux and regeneration of  $\text{MnO}_{2\text{-bio}}$  was relevant for effective BPA degradation. Manganese is the second most abundant transition metal in the Earth's crust, and a number of phylogenetically distinct Mn(II)-oxidizing bacteria and fungi have been identified in soil, sediment and aquatic environments.<sup>34</sup> The new findings, combined with previous  $\text{MnO}_{2\text{-syn}}$  studies, suggest that Mn(II) oxidation and  $\text{MnO}_{2\text{-bio}}$  formation may play relevant roles in controlling the fate and longevity of BPA in the environment including the subsurface environment. A future research focus should be on the interplay between microbial Mn(II) oxidation and mineral phase-mediated contaminant degradation, which can lead to innovative engineering approaches that capitalize on the BMAD concept.

## Chapter 3 - The relative roles of Mn(III) and Mn(IV) in BPA

### degradation by Mn-oxides

#### 3.1 Introduction

In nature, manganese prevails as Mn(II), Mn(III) and Mn(IV).<sup>34</sup> Mn(II) exists as soluble cation and Mn(IV) occurs as insoluble Mn-oxides (MnO<sub>2</sub>). MnO<sub>2</sub> formation is mainly attributed to microbial Mn(II) oxidation,<sup>34</sup> which is a two sequential one-electron transfer process with dissolved Mn(III) as an intermediate.<sup>50</sup> Because of this, MnO<sub>2</sub> produced by Mn(II) oxidation mostly exist as Mn(III) rich Mn(III/IV) oxide in nature. Mn(III) is very unstable and disproportionate into Mn(II) or Mn(IV) in aqueous solution.<sup>34,92</sup> Dissolved Mn(III) remains stable in the presence of ligands.<sup>34,53-55</sup> In natural environment, various microbes have been reported to produce ligands stabilizing Mn(III).<sup>55,56</sup> In laboratory settings, different ligands, such as pyrophosphate, EDTA, and citrate have been used to promote Mn(III) stability by forming Mn(III)-ligand complex.<sup>51,53,54</sup>

Synthetic and biogenic MnO<sub>2</sub>s have been reported to contain 20 to 37%<sup>33</sup> and 9 to 34%<sup>44,52</sup> of Mn(III) content respectively. Studies that showed the transformation of organic contaminants with Mn(III) was performed using Mn(III) rich MnO<sub>2-syn</sub>,<sup>57,58</sup> naturally occurring (biogenic) Mn(III/IV) oxides<sup>41</sup> and soluble Mn(III) complexes.<sup>53</sup> Although dissolved Mn(III) have been considered as a potent environmental oxidant, relative contribution Mn(III) in MnO<sub>2</sub> in the degradation of compounds, that are susceptible to only MnO<sub>2</sub> mediated degradation, such as BPA, are not elucidated.

In this study, we examined the relative role of Mn(III) and Mn(IV) in biogenic and synthetic MnO<sub>2</sub> having similar structures. A Mn(II) oxidizing bacterium, *Roseobacter* sp. AzwK-3b was used for

the production of biogenic  $\text{MnO}_{2\text{-bio}}$ . Mn(II) oxidation by *R. AzwK-3b* is mediated by extracellular superoxide production, and thus Mn(II) oxidizing activity can be maintained in cell-free filtrate.<sup>44,68</sup>  $\text{MnO}_{2\text{-bio}}$  produced by the cell-free (cf) filtrate is highly reactive colloidal birnessite-like phase with hexagonal symmetry.<sup>52,82</sup> They are highly disordered, nanocrystalline, phylломanganate phase with large surface areas and vacancy sites.<sup>81</sup> Cell free colloidal (cf-C)  $\text{MnO}_{2\text{-bio}}$  goes through structural ripening and transforms into cell free particulate (cf-P)  $\text{MnO}_{2\text{-bio}}$  which has a structure similar to triclinic birnessite.<sup>52</sup> The goal of this study was to identify the role of Mn(III) and Mn(IV) in both of the cf- $\text{MnO}_{2\text{-bio}}$  and their synthetic counterparts, hexagonal and triclinic birnessite.

## **3.2 Materials and Methods**

### ***3.2.1 Chemicals and $\text{MnO}_2$ preparation***

Mn(III) acetate dihydrate was bought from Sigma-Aldrich. Two different  $\text{MnO}_2$  were synthesized according to methods described elsewhere. Hexagonal birnessite was synthesized by adding 6.9 mL of concentrated (36%) hydrochloric acid (dropwise) to a boiling solution of 100 mL 0.4 M potassium permanganate.<sup>93</sup> After boiling for ten more minutes the precipitate was collected. Triclinic birnessite was synthesized by mixing 200 mL of 0.5 M  $\text{MnCl}_2$  with 250 mL of 5.5 M NaOH. The Mixture was oxygenated for about five hours at a rate of  $1.5 \text{ L min}^{-1}$  using a diffusing stone.<sup>94</sup> Both  $\text{MnO}_2$  particles were collected and washed five times with DI water before storing.

### ***3.2.2 Preparation of cell free biogenic $\text{MnO}_{2\text{-bio}}$***

Cultures of *R. AzwK-3b* were grown at  $30^\circ\text{C}$  to early stationary phase in K medium (2 g/L peptone, 0.5 g/L yeast extract, and 20 mM HEPES buffer, pH 7.5) prepared with 75% (volume) artificial seawater (K-ASW))<sup>95</sup> and centrifuged at 12100 rpm for 10 minutes. The cell free supernatant was

filtered through a 0.22  $\mu\text{m}$  PVDF filter [MilliporeSigma™ Stericup™ Quick Release-HV Vacuum Filtration System] followed by the addition of 100  $\mu\text{M}$   $\text{MnCl}_2$  to the filtrate.<sup>74</sup> cf-C and cf-P  $\text{MnO}_2\text{-bio}$  were harvested by centrifuging at 12100 rpm for 25 minutes after 24 hours and 96 hours of incubation, respectively (Figure 3.1). The amount of  $\text{MnO}_2\text{-bio}$  was quantified by colorimetric LBB assay<sup>76</sup> in all four samples – synthetic (hexagonal and triclinic birnessite) and biogenic (cf-C and cf-P)  $\text{MnO}_2$ .

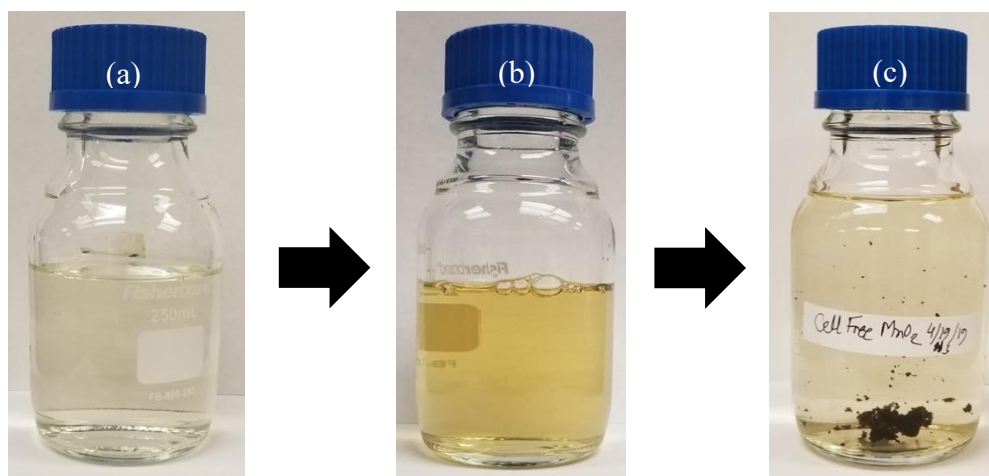


**Figure 3.1 Cell free  $\text{MnO}_2\text{-bio}$  formation (a) Control, (b) cf-C  $\text{MnO}_2\text{-bio}$ , (c) cf-P  $\text{MnO}_2\text{-bio}$ .**

### ***3.2.3 Mn(III)-pyrophosphate complex preparation and measurement***

Mn(III) acetate was added to anoxic sodium pyrophosphate (Na-PP) at different concentrations to prepare Mn(III)-pyrophosphate (Mn(III)-PP) complex solution of different ligand to Mn(III) ratios. Mn(III) content in cf-C  $\text{MnO}_2\text{-bio}$ , cf-P  $\text{MnO}_2\text{-bio}$  hexagonal and triclinic birnessite was measured by observing the absorbance of Mn(III)-PP complex concentration at 258 nm (Mn(III)-PP complex shows a maximum absorbance at 258 nm wavelength) using UV-Vis spectrophotometer. Samples were filtered and diluted 10 times before measuring the absorbance. The absorbance were converted to concentrations using extinction coefficient. By developing a standard curve with different known amounts of Mn(III)-PP complex, the extinction coefficient of  $6.97 \text{ mM}^{-1}\text{cm}^{-1}$  was

measured which is compatible with published value of  $6.75 \text{ mM}^{-1}\text{cm}^{-1}$ .<sup>79,96</sup> After adding PP, concentrations of the four  $\text{MnO}_2$ s were measured by LBB assay.

#### ***3.2.4 Mn(III) extraction from $\text{MnO}_{2\text{-syn}}$***

Mn(III) was extracted from  $\text{MnO}_{2\text{-syn}}$  (triclinic birnessite) by a method mentioned elsewhere<sup>57</sup>. In brief, 3 mM of triclinic birnessite was suspended in 250 mL of 50 mM PP and stirred up to 3 days. After 3 days, the suspension was filtered through 0.22  $\mu\text{m}$  filter paper and Mn(III)-PP concentration was quantified using extinction coefficient measured in the previous section. The Mn(III) free hexagonal and triclinic birnessite were prepared by the same extraction method. Briefly, 3 mM of hexagonal and triclinic birnessite were suspended in containing 250 mL of 50 mM PP and stirred up to 3 days. After 3 days, the suspension was filtered through 0.22  $\mu\text{m}$  glass fiber filter paper and the Mn(III) content was discarded. The filter papers containing Mn(IV) were suspended in DI water followed by discarding the filter papers from the suspension. Their nominal concentration was quantified with LBB assay.

#### ***3.2.5 BPA degradation kinetics***

BPA degradation kinetics were measured for cf-C  $\text{MnO}_{2\text{-bio}}$ , cf-P  $\text{MnO}_{2\text{-bio}}$  and  $\text{MnO}_{2\text{-synS}}$  (hexagonal and triclinic birnessite). To examine BPA degradation with cf  $\text{MnO}_{2\text{-bio}}$ , experiments were conducted in a total volume of 10 mL with 44  $\mu\text{M}$  (10 mg/L) and 18  $\mu\text{M}$  (4 mg/L) of BPA in 5 mM phosphate buffer in the absence and presence of 5 mM sodium pyrophosphate respectively at pH 7. BPA degradation experiments were initiated by adding cf  $\text{MnO}_{2\text{-bio}}$  into the vessels to achieve a concentration of 0.2 mM. Effect of  $\text{MnO}_{2\text{-syn}}$ -hexagonal and triclinic birnessite loading on BPA was examined by conducting experiment in a total volume of 50 mL with 18  $\mu\text{M}$  (4 mg/L) BPA in 5 mM phosphate buffer in the presence and absence of 5 mM sodium pyrophosphate at

pH 7. Mn(III) free  $\text{MnO}_{2\text{-syn}}$  were also examined with 44  $\mu\text{M}$  (10 mg/L) BPA in a total volume of 50 mL 5 mM phosphate buffer without PP. Effect of Mn(III)-PP complex with various ligand concentrations (1, 5, 10 mM) on BPA was examined separately with 44  $\mu\text{M}$  BPA in 50 mL volume. Mn(III)-PP extracted from triclinic birnessite (having a ligand concentration of 5mM) was also incubated with BPA in similar experimental setup. In all the experiments  $\text{MnO}_2$  and Mn(III)-PP complex concentration was 0.2 mM. Aliquots (50  $\mu\text{L}$ ) of the mixture was periodically collected and transferred to HPLC vial inserts containing 2  $\mu\text{L}$  of L-ascorbic acid solution (50 mg  $\text{mL}^{-1}$ ) and vigorously mixed with a vortex mixer. Ascorbic acid converts any remaining  $\text{MnO}_2$  to Mn(II) ions and quenches the reaction.<sup>27,42</sup> An Agilent 1200 Series HPLC equipped with a fluorescence detector (FLD) was used for the detection and quantification of BPA and HCA as mentioned in section 2.2.4.

### **3.3 Results**

#### ***3.3.1 Abiotic BPA degradation with cell free biogenic and synthetic $\text{MnO}_2$***

To examine the effect of Mn(III) in BPA degradation abiotic BPA degradation experiments were conducted in the presence and absence of PP. When BPA was incubated with cf-C  $\text{MnO}_{2\text{-bio}}$  and cf-P  $\text{MnO}_{2\text{-bio}}$  without PP, BPA disappearance was not observed at pH 7 (Figure 3.2 a). However, BPA was degraded when this experiment was conducted without PP at pH 4 (Figure 3.2 c). Again, when BPA was incubated with cf-C  $\text{MnO}_{2\text{-bio}}$  and cf-P  $\text{MnO}_{2\text{-bio}}$  in the presence of PP at pH 7, both cf-C  $\text{MnO}_{2\text{-bio}}$  and cf-P  $\text{MnO}_{2\text{-bio}}$  degraded BPA (Figure 3.2 b). BPA removal rate of 0.03  $\text{min}^{-1}$  and 0.01  $\text{min}^{-1}$  was observed with cf-C  $\text{MnO}_{2\text{-bio}}$  and cf-P  $\text{MnO}_{2\text{-bio}}$  respectively in the presence of PP (Figure 3.2 b; Table 3.1). The BPA degradation rates of hexagonal birnessite in the presence and absence of PP were similar (0.006  $\text{min}^{-1}$  and 0.007  $\text{min}^{-1}$ , respectively) (Figure 3.3 a, b; Table

3.1). However, BPA degradation rate by triclinic birnessite increased more than 10-fold in the presence of PP ( $0.006 \text{ min}^{-1}$ ) than in the absence of PP ( $0.0007 \text{ min}^{-1}$ ) (Figure 3.3 a, b; Table 3.1).

**Table 3.1 BPA degradation rates for synthetic and biogenic MnO<sub>2</sub>.**

MnO <sub>2</sub>	BPA degradation rates (min <sup>-1</sup> )		
	pH 7 without PP	pH 4 without PP	pH 7 with PP
cf-C MnO <sub>2-bio</sub>	x	0.014 ± 0.001	0.03 ± 0.003
cf-P MnO <sub>2-bio</sub>	x	0.01 ± 0.0007	0.01 ± 0.0007
Hexagonal Birnessite	0.006 ± 0.0004	X	0.007 ± 0.0007
Triclinic birnessite	0.0007 ± 0.0001	X	0.006 ± 0.0007
Mn(III) free Hexagonal Birnessite	0.004 ± 0.001	X	x
Mn(III) free Triclinic Birnessite	0.0006 ± 0.0001	X	x

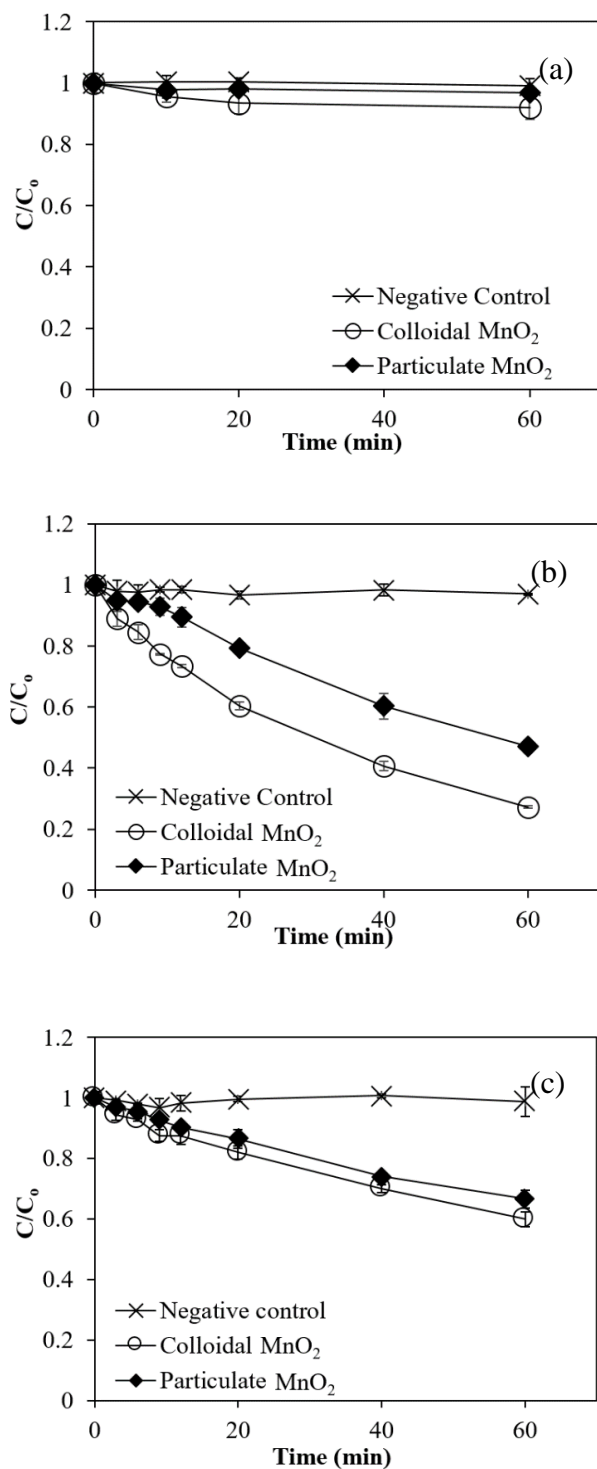


**Figure 3.2 BPA degradation with 0.2 mM cf-C  $MnO_2$ -bio and cf-P  $MnO_2$ -bio, (a) without PP at pH 7 (b) with PP at pH 7 (c) without PP at pH 4. Error bars represent the standard deviation of triplicate samples. Error bars smaller than the symbol size are not depicted.**

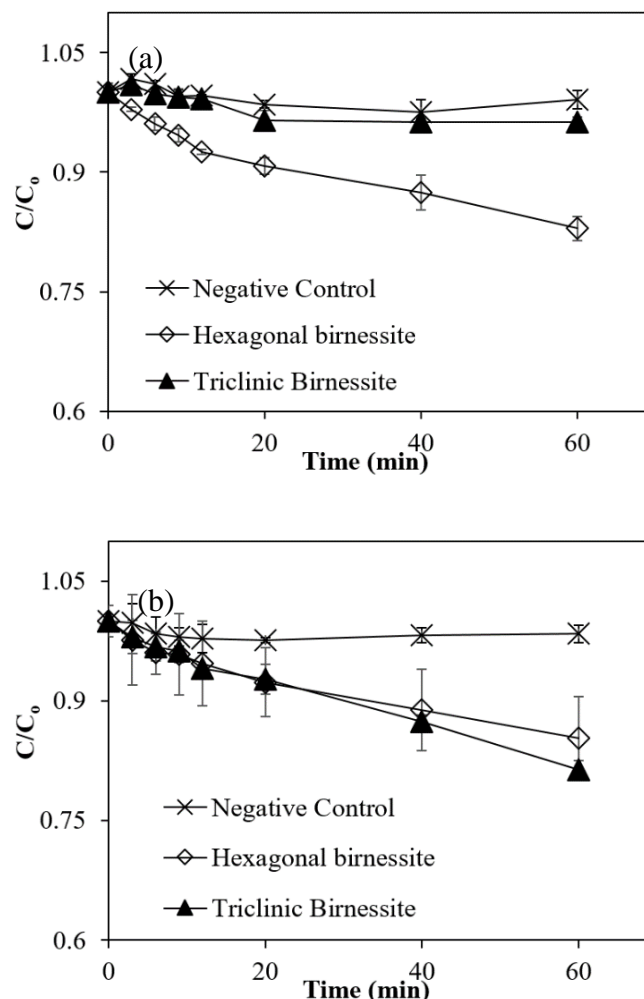


**Figure 3.3 BPA degradation with 0.2 mM  $MnO_{2-syn}$  (a) without PP at pH 7 (b) with PP at pH 7. Error bars represent the standard deviation of triplicate samples. Error bars smaller than the symbol size are not depicted.**

To examine the role of only Mn(IV), BPA degradation experiment was conducted with Mn(III) free  $MnO_{2-syn}$  (Figure 3.4). BPA degradation rates with hexagonal birnessite was  $0.004 \text{ min}^{-1}$  that was close to the BPA degradation rate ( $0.007 \text{ min}^{-1}$ ) with hexagonal birnessite in the absence of PP (Table 3.1). For triclinic birnessite also, degradation rates with Mn(III) free and without PP condition were similar ( $0.0007 \text{ min}^{-1}$  and  $0.0006 \text{ min}^{-1}$  respectively) (Figure 3.4; Table 3.1). BPA degradation for all  $MnO_2$  are summarized in table 3.1. For all the experiments, BPA degradation was not observed in negative control incubations.

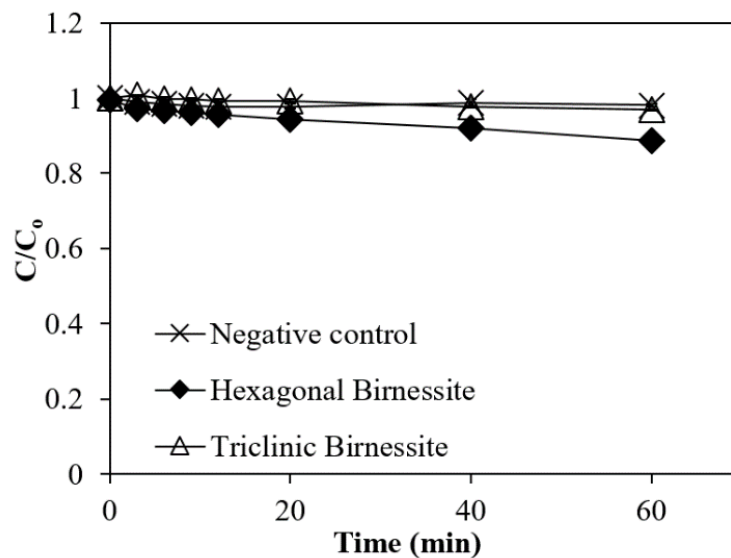


**Figure 3.4 BPA degradation with 0.2 mM  $\text{MnO}_{2\text{-syn}}$  free of Mn(III). Error bars represent the standard deviation of triplicate samples. Error bars smaller than the symbol size are not depicted.**

### 3.3.2 Mn (III) availability in different MnO<sub>2</sub>

Mn(III)-PP has a typical absorbance peak at 258 nm.<sup>79,96</sup> To calculate the molar extinction coefficient of Mn(III)-PP at 258 nm, a standard curve of absorbance vs Mn(III)-PP complex was developed by measuring the absorbance of known concentrations (5, 10, 30, 50 and 100 μM) of Mn(III) acetate-PP complex (Figure 3.5). The molar extinction coefficient was calculated to be 6.97 mM<sup>-1</sup>cm<sup>-1</sup>.

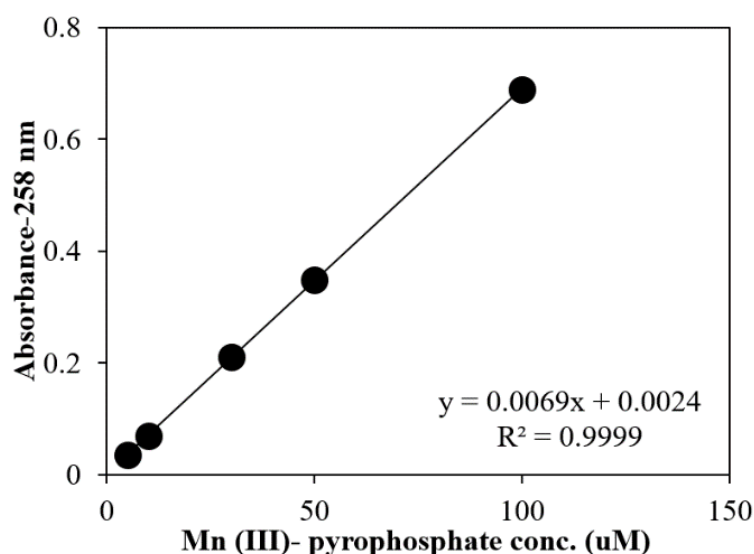


**Figure 3.5** An example of a Mn(III)-PP standard curve.

To examine the Mn(III) content in cf-C MnO<sub>2-bio</sub>, cf-P MnO<sub>2-bio</sub> and MnO<sub>2-syn</sub> (hexagonal and triclinic birnessite), Mn (III)-PP concentrations were measured over time (Figure 3.6). Table 3.2 shows the Mn(III) concentration at the end of the incubation, i.e., Mn(III) content, of different Mn-oxides. For cf-C MnO<sub>2-bio</sub> and cf-P MnO<sub>2-bio</sub>, more than 50% of the Mn(III) was released in one hour, whereas 2% and 25.4% Mn(III) was released from hexagonal and triclinic birnessite, respectively (Table 3.2). After six hours, Mn(III) contents in cf-C MnO<sub>2-bio</sub> and cf-P MnO<sub>2-bio</sub> were 64.2% and 62.7%, and those in hexagonal and triclinic birnessite were 2.8% and 36%, respectively

(Table 3.2). Mn(III) release rate from these data were calculated for all four MnO<sub>2</sub>s. Mn(III) release rate for cf-C MnO<sub>2-bio</sub>, cf-P MnO<sub>2-bio</sub>, hexagonal and triclinic birnessite were 0.125 min<sup>-1</sup>, 0.078 min<sup>-1</sup>, 0.005 min<sup>-1</sup> and 0.045 min<sup>-1</sup> respectively (Table 3.2). BPA degradation rates are correlated with Mn(III) release rate for all four MnO<sub>2</sub> which is shown in Figure 3.7.

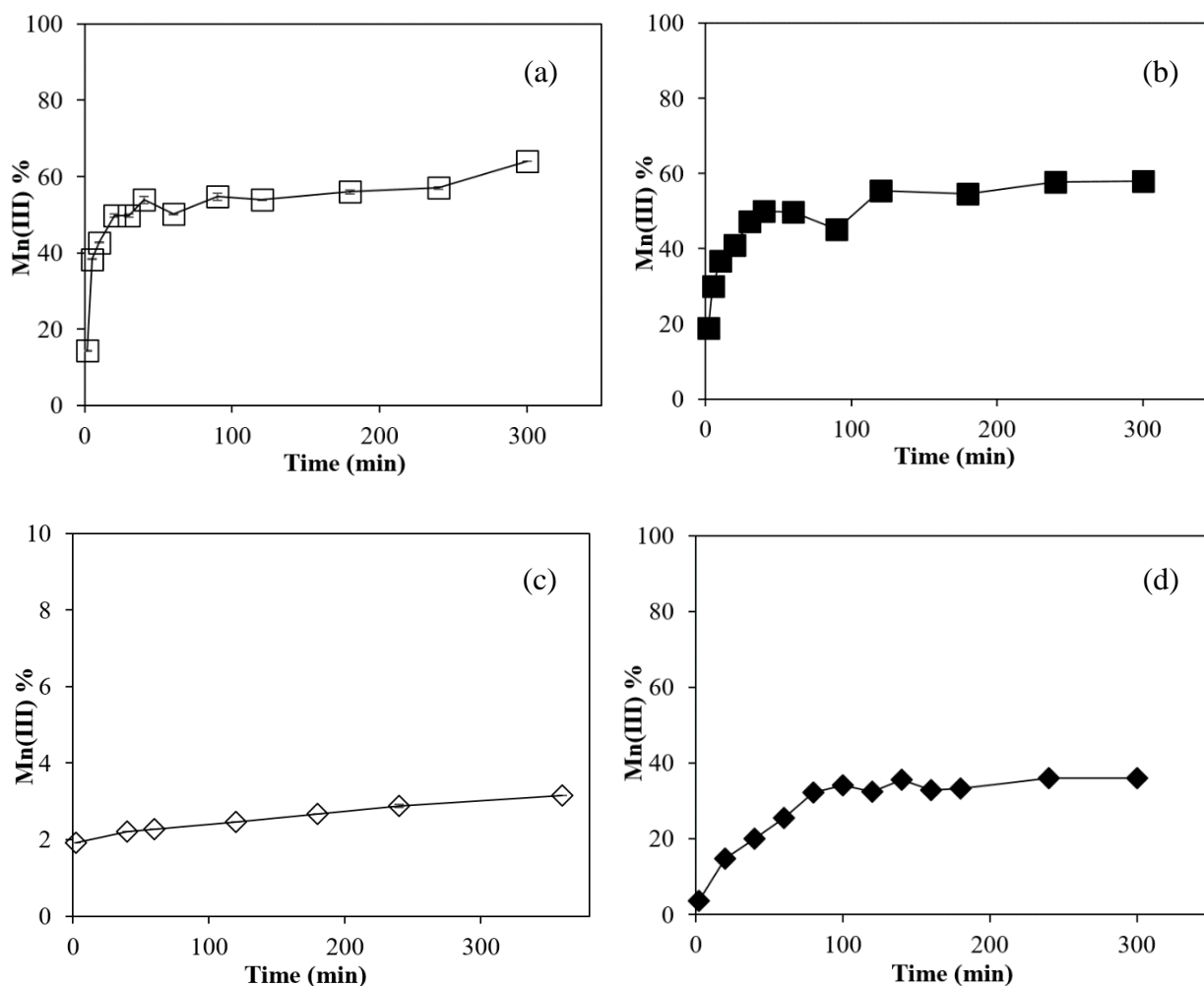


**Figure 3.6 Mn release rate for (a) cf-C MnO<sub>2-bio</sub>, (b) cf-P MnO<sub>2-bio</sub>, (c) hexagonal birnessite and (d) triclinic birnessite. Error bars represent the standard deviation of triplicate samples. Error bars smaller than the symbol size are not depicted.**

**Table 3.2 Mn(III) content and release rate from different MnO<sub>2</sub>.**

MnO <sub>2</sub>	Mn(III)% extracted after 2 minutes	Mn(III)% extracted after 60 minutes	Mn(III) (%) extracted after 6 hours	Mn(III) release rate (min <sup>-1</sup> )
cf-C MnO <sub>2</sub> -bio	14.33	50.1	64.2	0.125 ± 0.08
cf-P MnO <sub>2</sub> -bio	18.9	49.7	62.7	0.078 ± 0.03
Hexagonal birnessite	1.7	2.01	2.8	0.005 ± 0.0004
Triclinic birnessite	3.6	25.4	35.9	0.045 ± 0.018

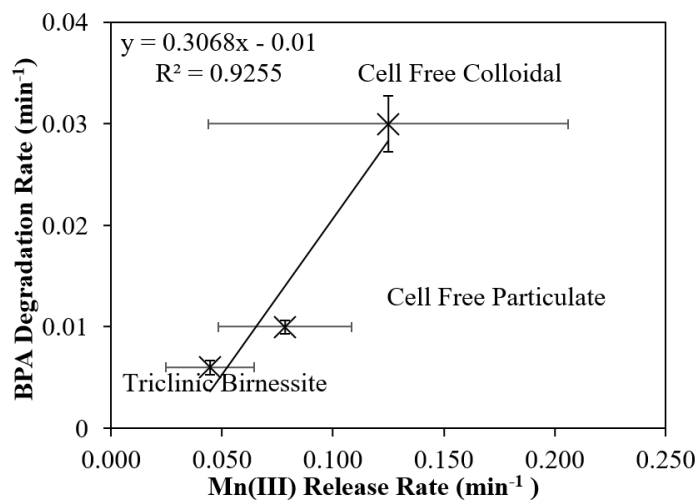


**Figure 3.7 BPA degradation rates vs Mn(III) content release rates in four MnO<sub>2</sub>. Error bars represent the standard deviation of triplicate samples.**

### ***3.3.3 BPA degradation by Mn(III) acetate -PP at different ligands and Mn(III) extracted from triclinic birnessite***

To examine the influence of ligand concentration on the BPA degradation rates, 44  $\mu\text{M}$  BPA was incubated with 0.2 mM Mn(III) acetate-PP complex at different ligand concentrations (1, 5, 10 mM) Figure 3.8 a shows that less BPA was removed with increasing pyrophosphate concentration. BPA removal rate of  $0.03 \pm 0.008 \text{ min}^{-1}$  was observed in the presence of 1 mM pyrophosphate and a 30 times slower rate of  $0.001 \text{ min}^{-1}$  was observed with 10 mM pyrophosphate (Figure 3.8 b; Table 3.3). BPA was also incubated with 0.2 mM Mn(III)-PP extracted from triclinic birnessite in the presence of 5mM PP and same experimental condition. This showed a BPA removal rate of  $0.007 \pm 0.001 \text{ min}^{-1}$  which is similar to that of pure Mn(III) acetate-PP ( $0.006 \pm 0.001 \text{ min}^{-1}$ ) (Figure 3.8; Table 3.3). BPA degradation rates for all Mn(III)-PP at different ligand concentrations are showed in table 3.3.

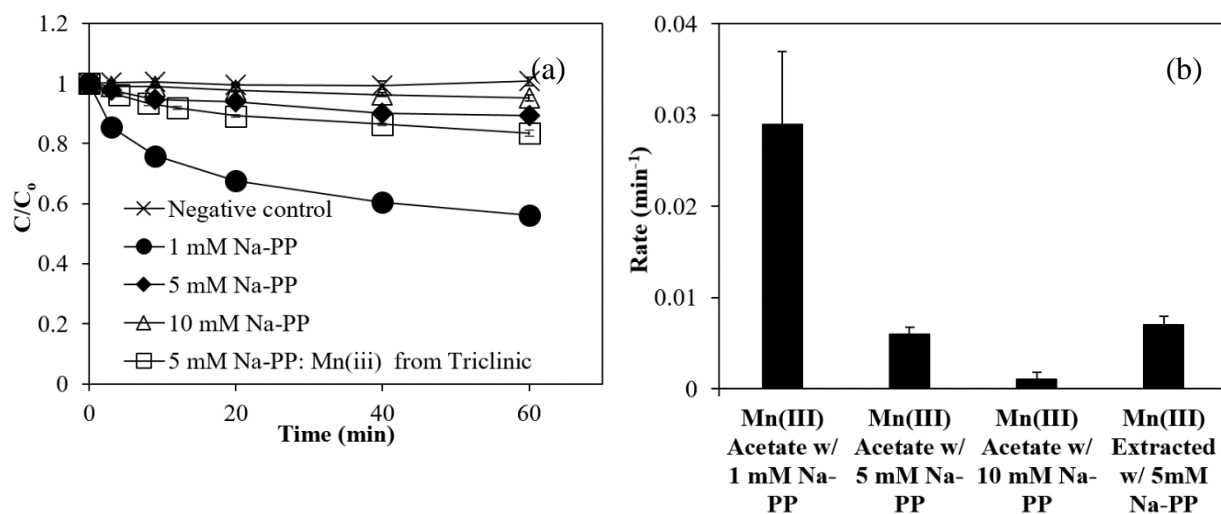


**Figure 3.8 (a) BPA degradation and (b) BPA degradation rates with 0.2 mM synthetic Mn(III) acetate-PP at different PP concentrations (Na-PP). The last legend is for Mn(III) extracted from triclinic birnessite. Error bars represent the standard deviation of triplicate samples. Error bars smaller than the symbol size are not depicted.**

**Table 3.3 BPA degradation rates for Mn(III) mediated BPA degradation experiments at different ligand concentration.**

Mn(III) type	Ligand concentration (mM)	BPA degradation rate ( $\text{min}^{-1}$ )
Synthetic Mn(III)	1	$0.03 \pm 0.008$
Synthetic Mn(III)	5	$0.006 \pm 0.0007$
Synthetic Mn(III)	10	$0.001 \pm 0.0008$
Mn(III) extracted from triclinic birnessite	5	$0.007 \pm 0.001$

### 3.4 Discussion

Mn(III) is an intermediate in the oxidation of Mn(II) oxidation to Mn(IV), which is a two one electron transfer process.<sup>50,51</sup> In nature, Mn(III) is complexed by organic complexing agents produced by them<sup>53</sup>. Mn(III) is a strong oxidant that is known to effectively oxidize phenol, sulfide,<sup>57</sup> triclosan<sup>97</sup> etc. Surface Mn(III) in different phase of MnO<sub>2-syn</sub> have been reported to play an important role in the reactivity of MnO<sub>2-syn</sub>.<sup>33</sup> However, relative role of Mn(III) and Mn(IV) in MnO<sub>2</sub> has not been assessed. The oxidation of Mn(II) by *Roseobacter* sp. AzwK-3b occurs in its cell-free spent medium.<sup>52,68,82</sup> After incubation with Mn(II), oxidation occurs (8-25 hours) which was visually apparent due to a golden color of cf-C MnO<sub>2-bio</sub> in the media and this was followed by formation of brown cf-P MnO<sub>2-bio</sub> particles (>48 hours). According to previous studies, cf-C MnO<sub>2-bio</sub> is structurally similar to hexagonal birnessite which ripens into is less reactive cf-P MnO<sub>2-bio</sub>, structurally similar to triclinic birnessite<sup>10</sup>. Due to their greater surface area and disordered structure, cf-MnO<sub>2-bio</sub>s are more reactive than their synthetic counterparts.<sup>80,81,98</sup> Reactivity of birnessite has been attributed to Mn(III) within the layers of the minerals<sup>99,100</sup> which is also applicable for cf-C MnO<sub>2-bio</sub> and cf-P MnO<sub>2-bio</sub> as shown by a previous study.<sup>52</sup>

cf-MnO<sub>2-bio</sub> is highly reactive and demonstrated oxidation of chromium. When cf-C MnO<sub>2-bio</sub> and cf-P MnO<sub>2-bio</sub> was incubated with BPA, BPA degradation was not observed (Figure 3.2 a). It was speculated that the cf-C MnO<sub>2-bio</sub> and cf-P MnO<sub>2-bio</sub> were not reactive towards BPA. However, degradation occurred for the same experimental conditions at pH 4. It is known that oxidation of organic compounds are pH dependent and exponentially increase at lower pH.<sup>42,101</sup> MnO<sub>2-syn</sub> mediated BPA degradation was also faster at lower pH.<sup>30</sup> This implies that cf-C MnO<sub>2-bio</sub> and cf-P MnO<sub>2-bio</sub> are reactive but the Mn(III) in them may have been transformed to Mn(II) or Mn(IV)

making them less reactive. It is known that aqueous Mn(III) ions are very unstable against disproportionation without ligands:<sup>53</sup>



Also, the Mn(IV) in cf-C MnO<sub>2-bio</sub> and cf-P MnO<sub>2-bio</sub> is clearly not as reactive as the synthetic MnO<sub>2-syn</sub>, vernadite, previously reported to degrade BPA.<sup>30</sup> BPA was incubated with hexagonal and triclinic birnessite without PP but BPA degradation rate was slower in triclinic birnessite (Figure 3.3 a). This suggests that, Mn(IV) may not be as reactive in triclinic as hexagonal birnessite. In the presence of pyrophosphate (PP), Mn(III) can be stabilized. When BPA was incubated with cf-C MnO<sub>2-bio</sub>, cf-P MnO<sub>2-bio</sub>, and triclinic birnessite in the presence of PP, BPA was degraded (Figure 3.2 b; Figure 3.3 b), although similar BPA degradation occurred for hexagonal birnessite in the presence and absence of PP. This suggests that the PP extracts and protects reactive Mn(III)-species and forms Mn(III)-PP complex from cf-C MnO<sub>2-bio</sub> and cf-P MnO<sub>2-bio</sub>. To observe the role of only Mn(IV) on BPA degradation synthetic MnO<sub>2</sub> were made Mn(III) free by extracting Mn(III) from them and incubating with BPA. The similar BPA degradation rates with pure and Mn(III) free synthetic MnO<sub>2</sub> speculates that Mn(III) is responsible for BPA degradation in triclinic birnessite whereas for hexagonal it is only Mn(IV).

Studies have emphasized the importance of Mn(III) content for oxidation of compounds when they are extracted using a ligand from the Mn-oxides<sup>57,58</sup>. Huang et al. suggested a strong positive correlation between Mn(III) content and reactivity in MnO<sub>2-syn</sub>.<sup>33</sup> We measured the Mn(III) content in cf-C MnO<sub>2-bio</sub> and cf-P MnO<sub>2-bio</sub> and their synthetic counterparts- hexagonal and triclinic birnessite and got much higher Mn(III) content in cf-C MnO<sub>2-bio</sub> and cf-P MnO<sub>2-bio</sub> than hexagonal and triclinic birnessite (Table 3.2). The Mn(III) content in hexagonal and triclinic birnessite are reported as 10%<sup>39</sup> and 20%<sup>102</sup> respectively and in this study we got 3% and 36% respectively. This

difference in Mn(III) content can be due to the different synthesizing techniques for these hexagonal and triclinic birnessite. A previous study has shown difference in Mn(III) content in same MnO<sub>2-syn</sub> for different synthesis procedures.<sup>33</sup>

In this study, lower Mn(III) in hexagonal birnessite can attribute to the similar BPA degradation with and without PP. However, for triclinic birnessite BPA degradation rates did not correlate with considerable amount of Mn(III) content in it, which was observed for both cf- MnO<sub>2-bio</sub>. This BPA degradation rates can be correlated to the Mn(III) release rate which was calculated by measuring Mn(III) content over time from all four MnO<sub>2</sub>. The rates of Mn(III) release from the MnO<sub>2</sub> have not been demonstrated previously which we believe is the key factor for Mn(III) availability for the degradation of BPA. Mn(III) release rate of 0.125 min<sup>-1</sup>, 0.078 min<sup>-1</sup>, 0.005 min<sup>-1</sup> and 0.045 min<sup>-1</sup> was observed for cf-C MnO<sub>2-bio</sub>, cf-P MnO<sub>2-bio</sub>, hexagonal and triclinic birnessite which correlates well with the BPA degradation rates (Figure 3.7). A previous study showed that even though Mn(III) content was similar in MnO<sub>2</sub> they have different reactivity.<sup>33</sup> This can be explained by the Mn(III) release rate from the cf-C MnO<sub>2-bio</sub> and cf-P MnO<sub>2-bio</sub> observed in this study. Therefore, even though structurally similar, Mn(III) content and release rate in synthetic and biogenic MnO<sub>2</sub> are not the same and as a result reactivity towards BPA degradation is also different.

Mn(III)-PP complex can equilibrate to free Mn(III)<sup>59</sup> that is believed to be responsible for BPA degradation. A previous study emphasized the importance of free Mn(III) from Mn(III)-PP on the degradation of organic contaminants.<sup>59</sup> However, PP exerts inhibitory effect through complexation on the surface of Mn-oxide.<sup>57</sup> When BPA was incubated with same concentration of Mn(III) acetate complexed at different pyrophosphate concentrations, higher concentration of pyrophosphate showed slower degradation mechanism (Figure 3.8). This may be due to the fact

that Mn(III) was crowded by high concentration of pyrophosphate making it less accessible to BPA by forming stronger Mn(III)-pyrophosphate complex and rendering less free Mn(III). Hu et al. reported that, PP complexation with Mn(III) rendered less available Mn(III) to bond with organic contaminant and thereby reducing degradation rates.<sup>59</sup> PP also affects the mobility of Mn species in nature and control the contribution of soluble Mn(III) content to a great extent.<sup>96</sup> This experiment was also repeated with same concentration of Mn(III)-PP complex extracted from triclinic birnessite and it showed a similar BPA degradation rates (Figure 3.8) suggesting that there is no difference in synthetic Mn(III)-complex and Mn(III)-complex extracted from synthetic Mn-oxides.

### **3.5 Environmental Implications**

BPA is present in anoxic sediments<sup>44,4</sup> that can be degraded in the presence of reactive mineral like MnO<sub>2</sub>. In nature, MnO<sub>2</sub> are mostly present as Mn(III/IV)-oxides. In laboratory settings, different type of Mn(III) rich MnO<sub>2-syn</sub> has demonstrated BPA degradation.<sup>33</sup> This study shows that depending on Mn(III) content and release rate, BPA degradation can be facilitated in MnO<sub>2</sub>. As amount of BPA discharged in the environment continue to grow, fate of BPA can be predicted further by giving importance to the relative role of Mn(III) and Mn(IV) in MnO<sub>2</sub> and taking Mn(III) release rate into consideration. We are hopeful that it can also lead to future studies of BPA degradation mechanism involving Mn(III) in live cultures in the presence of MnO<sub>2</sub>.

## Chapter 4 - Conclusion

This thesis aimed to explore the role of three manganese oxidizing bacteria (MOB) mediated abiotic BPA degradation in the presence of  $\text{MnO}_{2\text{-bio}}$  and the relative role of Mn(III) and Mn(IV) in  $\text{MnO}_2$ . Many studies have investigated  $\text{MnO}_{2\text{-syn}}$ -mediated BPA degradation,<sup>27-30,38</sup> but the relevance of these findings for *in situ* activity are not clear. Natural organic matter and metal ions affecting the mineral phase reactivity of  $\text{MnO}_2$  on BPA have also been assessed and demonstrated.<sup>27,29</sup> However, the combined assessment of microbial activity and related abiotic degradation has not received adequate attention. In the first study, three MOB having different Mn(II) oxidizing enzymes showed different BPA degradation trends in the presence of different amount of Mn(II). Low amount of Mn(II) e.g. 10  $\mu\text{M}$  Mn(II) showed high BPA degradation rates for all three bacteria. This suggests, lower amount of Mn(II) can be reused to produce  $\text{MnO}_{2\text{-bio}}$  to remove BPA to a great extent in the environment. However, higher Mn(II) is not always efficient in BPA degradation kinetics and can actually impede BPA degradation to some extent. In the environment, most of the  $\text{MnO}_2$  produced are the result of microbially catalyzed Mn(II) oxidation. This suggests, biologically mediated abiotic degradation (BMAD) of BPA concept is important in understanding BPA degradation better.

In the second study, the relative role of Mn(III) and Mn(IV) in both biogenic and synthetic and  $\text{MnO}_2$  is assessed. Dissolved Mn(III) can disproportionate into Mn(II) or Mn(IV) in aqueous solution.<sup>92</sup> and also become a part of  $\text{MnO}_2$  residing in the layer vacancy sites of the  $\text{MnO}_{2\text{-bio}}$ .<sup>44</sup> In nature, organic ligands stabilize Mn(III) which can be available for BPA degradation in the subsurface or aquatic environment. Depending on the Mn(III) content and release rate over time from the  $\text{MnO}_2$ , BPA degradation kinetics model can be developed for practical situations.

Assessing the role of Mn(III) and Mn(IV) in the MnO<sub>2</sub> reactivity, degradation kinetics for compounds that are susceptible to degradation by Mn-oxides other than BPA can also be evaluated. BPA and BPA transformed compounds are, and will remain, part of modern societies for decades to come, and so will the associated concerns, unless clear understanding about the fate and the longevity of BPA in environmental systems are fully assessed by further research. A variety of biotic and abiotic processes can contribute to BPA transformation, degradation, and also incorporation into solid matrices (e.g., soil, sediment) which have been identified and documented in the laboratory. Many questions about the ultimate fate of BPA and its metabolites in the environment are still remaining. Further information about degradation pathways and mechanisms, contributing organisms, enzymes and genes, as well as favorable geochemical conditions that accommodate degradation is needed. Given the widespread distribution of Mn(IV)-reducing and Mn(II)-oxidizing microorganisms in subsurface and aquatic environment, active Mn cycling occurring in oxic-anoxic transition zones may be hotspots for MnO<sub>2</sub>-mediated BPA degradation.

## References

- (1) Staples, C. a; Dom, P. B.; Klecka, G. M.; Sandra, T. O.; Harris, L. R. A Review of the Environmental Fate, Effects, and Exposures of Bisphenol A. *Chemosphere* **1998**, *36* (10), 2149–2173.
- (2) Crain, D. A.; Eriksen, M.; Iguchi, T.; Jobling, S.; Laufer, H.; LeBlanc, G. A.; Guillette, L. J. An Ecological Assessment of Bisphenol-A: Evidence from Comparative Biology. *Reprod. Toxicol.* **2007**, *24* (2), 225–239.
- (3) Rochester, J. R. Bisphenol A and Human Health: A Review of the Literature. *Reprod. Toxicol.* **2013**, *42*, 132–155.
- (4) Bisphenol-A – A Global Market Overview. *Ind. Expert.* **2017**, 1–194.
- (5) Cousins, I. T.; Staples, C. A.; Klečka, G. M.; Mackay, D. A Multimedia Assessment of the Environmental Fate of Bisphenol A. *Hum. Ecol. Risk Assess.* **2002**, *8* (5), 1107–1135.
- (6) Barnabé, S.; Brar, S. K.; Tyagi, R. D.; Beauchesne, I.; Surampalli, R. Y. Pre-Treatment and Bioconversion of Wastewater Sludge to Value-Added Products-Fate of Endocrine Disrupting Compounds. *Sci. Total Environ.* **2009**, *407* (5), 1471–1488.
- (7) Bogdan, D. Removal of Bisphenol A from Water Using Iron Oxide Adsorbents. *PhD Diss. Univ. of Illinois Chicago* **2012**.
- (8) Wozniak, A. L.; Bulayeva, N. N.; Watson, C. S. Xenoestrogens at Picomolar to Nanomolar Concentrations Trigger Membrane Estrogen Receptor- $\alpha$ -Mediated  $\text{Ca}^{2+}$  Fluxes and Prolactin Release in GH3/B6 Pituitary Tumor Cells. *Environ. Health Perspect.* **2005**, *113* (4), 431–439.
- (9) Lang, I. A.; Galloway, T. S.; Scarlett, A.; Henley, W. E.; Depledge, M.; Wallace, R. B.; Melzer, D. Association of UrinaryBisphenolAConcentration With Medical Disorders and Laboratory Abnormalities in Adults. *Jama* **2008**, *300* (11), 1303–1310.

- (10) Bolz, U.; Hagenmaier, H.; Körner, W. Phenolic Xenoestrogens in Surface Water, Sediments, and Sewage Sludge from Baden-Württemberg, South-West Germany. *Environ. Pollut.* **2001**, *115* (2), 291–301.
- (11) Heemken, O. .; Reincke, H.; Stachel, B.; Theobald, N. The Occurrence of Xenoestrogens in the Elbe River and the North Sea. *Chemosphere* **2001**, *45* (3), 245–259.
- (12) Fromme, H.; Kuchler, T.; Otto, T.; Pilz, K.; Müller, J.; Wenzel, A. Occurrence of Phthalates and Bisphenol A and F in the Environment. *Water Res.* **2002**, *36* (6), 1429–1438.
- (13) Klecka, G. M.; Staples, C. a; Clark, K. E.; Van der Hoeven, N.; Thomas, D. E.; Hentges, S. G. Exposure Analysis of Bisphenol A in Surface Water Systems in North America and Europe. *Environ. Sci. Technol.* **2009**, *43* (16), 6145–6150.
- (14) Lee, H. B.; Peart, T. E. Determination of Bisphenol A in Sewage Effluent and Sludge by Solid-Phase and Supercritical Fluid Extraction and Gas Chromatography/Mass Spectrometry. *J. AOAC Int.* **2000**, *83* (2), 290–297.
- (15) Kolpin, D. W.; Furlong, E. T.; Meyer, M. T.; Thurman, E. M.; Zaugg, S. D.; Barber, L. B.; Buxton, H. T. Pharmaceuticals, Hormones, and Other Organic Wastewater Contaminants in U.S. Streams, 1999-2000: A National Reconnaissance. *Environ. Sci. Technol.* **2002**, *36* (6), 1202–1211.
- (16) Yamamoto, T.; Yasuhara, A.; Shiraishi, H.; Nakasugi, O. Bisphenol A in Hazardous Waste Landfill Leachates. *Chemosphere* **2001**, *42* (4), 415–418.
- (17) Robinson, B. J.; Hui, J. P. M.; Soo, E. C.; Hellou, J. Estrogenic Compounds in Seawater and Sediment from Halifax Harbour, Nova Scotia, Canada. *Environ. Toxicol. Chem.* **2009**, *28* (1), 18–25.
- (18) Melcer, H.; Klečka, G. Treatment of Wastewaters Containing Bisphenol A: State of the Science Review. *Water Environ. Res.* **2011**, *83* (7), 650–666.

- (19) Kalmykova, Y.; Björklund, K.; Strömvall, A. M.; Blom, L. Partitioning of Polycyclic Aromatic Hydrocarbons, Alkylphenols, Bisphenol A and Phthalates in Landfill Leachates and Stormwater. *Water Res.* **2013**, *47* (3), 1317–1328.
- (20) Ye, X.; Wong, L. Y.; Kramer, J.; Zhou, X.; Jia, T.; Calafat, A. M. Urinary Concentrations of Bisphenol A and Three Other Bisphenols in Convenience Samples of U.S. Adults during 2000-2014. *Environ. Sci. Technol.* **2015**, *49* (19), 11834–11839.
- (21) Im, J.; Löffler, F. E. Fate of Bisphenol A in Terrestrial and Aquatic Environments. *Environ. Sci. Technol.* **2016**, *50* (16), 8403–8416.
- (22) Zhang, W.; Yin, K.; Chen, L. Bacteria-Mediated Bisphenol A Degradation. *Appl. Microbiol. Biotechnol.* **2013**, *97* (13), 5681–5689.
- (23) Kang, J.-H.; Kondo, F. Bisphenol A Degradation by Bacteria Isolated from River Water. *Arch. Environ. Contam. Toxicol.* **2002**, *43* (3), 265–269.
- (24) Voordeckers, J. W.; Fennell, D. E.; Jones, K.; Häggblom, M. M. Anaerobic Biotransformation of Tetrabromobisphenol A, Tetrachlorobisphenol A, and Bisphenol A in Estuarine Sediments. *Environ. Sci. Technol.* **2002**, *36* (4), 696–701.
- (25) Kang, J. H.; Kondo, F. Bisphenol A Degradation in Seawater Is Different from That in River Water. *Chemosphere* **2005**, *60* (9), 1288–1292.
- (26) Im, J.; Prevatte, C. W.; Lee, H. G.; Campagna, S. R.; Löffler, F. E. 4-Methylphenol Produced in Freshwater Sediment Microcosms Is Not a Bisphenol A Metabolite. *Chemosphere* **2014**, *117* (1), 521–526.
- (27) Lin, K.; Liu, W.; Gan, J. Oxidative Removal of Bisphenol A by Manganese Dioxide: Efficacy, Products, and Pathways. *Environ. Sci. Technol.* **2009**, *43* (10), 3860–3864.
- (28) Gao, N.; Hong, J.; Yu, Z.; Peng, P.; Huang, W. Transformation of Bisphenol A in the Presence of Manganese Dioxide. *Soil Sci.* **2011**, *176* (6), 265–272.

- (29) Lin, K.; Peng, Y.; Huang, X.; Ding, J. Transformation of Bisphenol A by Manganese Oxide-Coated Sand. *Environ. Sci. Pollut. Res.* **2013**, *20* (3), 1461–1467.
- (30) Im, J.; Prevatte, C. W.; Campagna, S. R.; Löffler, F. E. Identification of 4-Hydroxycumyl Alcohol as the Major MnO<sub>2</sub>-Mediated Bisphenol A Transformation Product and Evaluation of Its Environmental Fate. *Environ. Sci. Technol.* **2015**, *49* (10), 6214–6221.
- (31) Balgooyen, S.; Alaimo, P. J.; Remucal, C. K.; Ginder-Vogel, M. Structural Transformation of MnO<sub>2</sub> during the Oxidation of Bisphenol A. *Environ. Sci. Technol.* **2017**, *51* (11), 6053–6062.
- (32) Balgooyen, S.; Campagnola, G.; Remucal, C. K.; Ginder-Vogel, M. Impact of Bisphenol A Influent Concentration and Reaction Time on MnO<sub>2</sub> Transformation in a Stirred Flow Reactor. *Environ. Sci. Process. Impacts* **2019**, *21* (1), 19–27.
- (33) Huang, J.; Zhong, S.; Dai, Y.; Liu, C. C.; Zhang, H. Effect of MnO<sub>2</sub> Phase Structure on the Oxidative Reactivity toward Bisphenol A Degradation. *Environmental Science and Technology*. **2018**, 11309–11318.
- (34) Tebo, B. M.; Bargar, J. R.; Clement, B. G.; Dick, G. J.; Murray, K. J.; Parker, D.; Verity, R.; Webb, S. M. Biogenic Manganese Oxides: Properties and Mechanisms of Formation. *Annu. Rev. Earth Planet. Sci.* **2004**, *32* (1), 287–328.
- (35) Nakamura, S.; Tezuka, Y.; Ushiyama, A.; Kawashima, C.; Kitagawara, Y.; Takahashi, K.; Ohta, S.; Mashino, T. Ipso Substitution of Bisphenol A Catalyzed by Microsomal Cytochrome P450 and Enhancement of Estrogenic Activity. *Toxicol. Lett.* **2011**, *203* (1), 92–95.
- (36) Zhu, M.; Ginder-Vogel, M.; Sparks, D. L. Ni(II) Sorption on Biogenic Mn-Oxides with Varying Mn Octahedral Layer Structure. *Environ. Sci. Technol.* **2010**, *44* (12), 4472–4478.
- (37) Villalobos, M.; Bargar, J.; Sposito, G. Trace Metal Retention on Biogenic Manganese Oxide Nanoparticles. *Elements* **2005**, *1* (4), 223–226.

- (38) Remucal, C. K.; Ginder-Vogel, M. A Critical Review of the Reactivity of Manganese Oxides with Organic Contaminants. *Environ. Sci. Process. Impacts* **2014**, *16* (6), 1247.
- (39) Sherman, D. M.; Peacock, C. L. Surface Complexation of Cu on Birnessite ( $\delta$ -MnO<sub>2</sub>): Controls on Cu in the Deep Ocean. *Geochim. Cosmochim. Acta* **2010**, *74* (23), 6721–6730.
- (40) Cheney, M. A.; Shin, J. Y.; Crowley, D. E.; Alvey, S.; Malengreau, N.; Sposito, G. Atrazine Dealkylation on a Manganese Oxide Surface. *Colloids Surfaces A Physicochem. Eng. Asp.* **1998**, *137* (1–3), 267–273.
- (41) Stone, A. T. Reductive Dissolution of Manganese(III/IV) Oxides by Substituted Phenols. *Environ. Sci. Technol.* **1987**, *21* (10), 979–988.
- (42) Zhang, H.; Huang, C. H. Oxidative Transformation of Triclosan and Chlorophene by Manganese Oxides. *Environ. Sci. Technol.* **2003**, *37* (11), 2421–2430.
- (43) Zhang, H.; Chen, W. R.; Huang, C. H. Kinetic Modeling of Oxidation of Antibacterial Agents by Manganese Oxide. *Environ. Sci. Technol.* **2008**, *42* (15), 5548–5554.
- (44) Learman, D. R.; Voelker, B. M.; Vazquez-Rodriguez, A. I.; Hansel, C. M. Formation of Manganese Oxides by Bacterially Generated Superoxide. *Nat. Geosci.* **2011**, *4* (2), 95–98.
- (45) Ehrlich, H. L.; Salerno, J. C. Energy Coupling in Mn<sup>2+</sup> Oxidation by a Marine Bacterium. *Arch. Microbiol.* **1990**, *154* (1), 12–17.
- (46) Kepkay, P. E.; Nealson, K. H. Growth of a Manganese Oxidizing Pseudomonas Sp. in Continuous Culture. *Arch. Microbiol.* **1987**, *148* (1), 63–67.
- (47) Anderson, C. R.; Johnson, H. A.; Caputo, N.; Davis, R. E.; Torpey, J. W.; Tebo, B. M. Mn(II) Oxidation Is Catalyzed by Heme Peroxidases in “Aurantimonas Manganoxydans” Strain SI85-9A1 and Erythrobacter Sp. Strain SD-21. *Appl. Environ. Microbiol.* **2009**, *75* (12), 4130–4138.
- (48) Geszvain, K.; Smesrud, L.; Tebo, B. M. Identification of a Third Mn(II) Oxidase Enzyme in Pseudomonas Putida GB-1. *Appl. Environ. Microbiol.* **2016**, *82* (13), 3774–3782.

- (49) Sakurai, T.; Kataoka, K. Basic and Applied Features of Multicopper Oxidases, Cueo, Bilirubin Oxidase, and Laccase. *Chem. Rec.* **2007**, *7* (4), 220–229.
- (50) Luther, G. W. Manganese(II) Oxidation and Mn(IV) Reduction in the Environment - Two One-Electron Transfer Steps versus a Single Two-Electron Step. *Geomicrobiol. J.* **2005**, *22* (3–4), 195–203.
- (51) Webb, S. M.; Dick, G. J.; Bargar, J. R.; Tebo, B. M. Evidence for the Presence of Mn(III) Intermediates in the Bacterial Oxidation of Mn(II). *Proc. Natl. Acad. Sci. U. S. A.* **2005**, *102* (15), 5558–5563.
- (52) Learman, D. R.; Wankel, S. D.; Webb, S. M.; Martinez, N.; Madden, A. S.; Hansel, C. M. Coupled Biotic-Abiotic Mn(II) Oxidation Pathway Mediates the Formation and Structural Evolution of Biogenic Mn Oxides. *Geochim. Cosmochim. Acta* **2011**, *75* (20), 6048–6063.
- (53) Kostka, J. E.; Luther, G. W.; Nealson, K. H. Chemical and Biological Reduction of Mn (III)-Pyrophosphate Complexes: Potential Importance of Dissolved Mn (III) as an Environmental Oxidant. *Geochim. Cosmochim. Acta* **1995**, *59* (5), 885–894.
- (54) Kenneth Klewicki, J.; Morgan, J. J. Kinetic Behavior of Mn(III) Complexes of Pyrophosphate, EDTA, and Citrate. *Environ. Sci. Technol.* **1998**, *32* (19), 2916–2922.
- (55) Parker, D. L.; Sposito, G.; Tebo, B. M. Manganese(III) Binding to a Pyoverdine Siderophore Produced by a Manganese(II)-Oxidizing Bacterium. *Geochim. Cosmochim. Acta.* **2004**, *68* (23), 4809–4820.
- (56) Johnson, H. A.; Tebo, B. M. In Vitro Studies Indicate a Quinone Is Involved in Bacterial Mn(II) Oxidation. *Arch. Microbiol.* **2008**, *189* (1), 59–69.
- (57) Nico, P. S.; Zamoski, R. J. Mn(III) Center Availability as a Rate Controlling Factor in the Oxidation of Phenol and Sulfide on  $\delta$ -MnO<sub>2</sub>. *Environ. Sci. Technol.* **2001**, *35* (16), 3338–3343.
- (58) Nico, P. S.; Zamoski, R. J. Importance of Mn(III) Availability on the Rate of Cr(III) Oxidation on  $\delta$ -MnO<sub>2</sub>. *Environ. Sci. Technol.* **2000**, *34* (16), 3363–3367.

- (59) Hu, E.; Zhang, Y.; Wu, S.; Wu, J.; Liang, L.; He, F. Role of Dissolved Mn(III) in Transformation of Organic Contaminants: Non-Oxidative versus Oxidative Mechanisms. *Water Res.* **2017**, *111* (Iii), 234–243.
- (60) Xyla, A. G.; Sulzberger, B.; Luther, G. W.; Hering, J. G.; Van Cappellen, P.; Stumm, W. Reductive Dissolution of Manganese(III,IV) (Hydr)Oxides by Oxalate: The Effect of PH and Light. *Langmuir* **1992**, *8* (1), 95–103.
- (61) Banerjee, D.; Nesbitt, H. W. XPS Study of Dissolution of Birnessite by Humate with Constraints on Reaction Mechanism. *Geochim. Cosmochim. Acta* **2001**, *65* (11), 1703–1714.
- (62) Tang, Y.; Webb, S. M.; Estes, E. R.; Hansel, C. M. Chromium(Iii) Oxidation by Biogenic Manganese Oxides with Varying Structural Ripening. *Environ. Sci. Process. Impacts* **2014**, *16* (9), 2127–2136.
- (63) Im, J.; Walshe-langford, G. E.; Moon, J. Environmental Fate of the Next Generation Refrigerant 2,3,3,3- Tetra Fl Uoropropene (HFO-1234yf). **2014**.
- (64) He, Y. T.; Wilson, J. T.; Su, C.; Wilkin, R. T. Review of Abiotic Degradation of Chlorinated Solvents by Reactive Iron Minerals in Aquifers. *Groundw. Monit. Remediat.* **2015**, *35* (3), 57–75.
- (65) Shaikh, N.; Taujale, S.; Zhang, H.; Artyushkova, K.; Ali, A. M. S.; Cerrato, J. M. Spectroscopic Investigation of Interfacial Interaction of Manganese Oxide with Triclosan, Aniline, and Phenol. *Environ. Sci. Technol.* **2016**, *50* (20), 10978–10987.
- (66) Miyata, N.; Tani, Y.; Sakata, M.; Iwahori, K. Microbial Manganese Oxide Formation and Interaction with Toxic Metal Ions. *J. Biosci. Bioeng.* **2007**, *104* (1), 1–8.
- (67) Geszvain, K.; Tebo, B. M. Identification of a Two-Component Regulatory Pathway Essential for Mn(II) Oxidation in Pseudomonas Putida GB-1. *Appl. Environ. Microbiol.* **2010**, *76* (4), 1224–1231.

- (68) Francis, C. A.; Co, E. M.; Tebo, B. M. Enzymatic Manganese(II) Oxidation by a Marine  $\alpha$ -Proteobacterium. *Appl. Environ. Microbiol.* **2001**, *67* (9), 4024–4029.
- (69) Im, J.; Walshe-Langford, G. E.; Moon, J. W.; Löffler, F. E. Environmental Fate of the next Generation Refrigerant 2,3,3,3-Tetrafluoropropene (HFO-1234yf). *Environ. Sci. Technol.* **2014**, *48* (22), 13181–13187.
- (70) De Rudder, J.; Van De Wiele, T.; Dhooge, W.; Comhaire, F.; Verstraete, W. Advanced Water Treatment with Manganese Oxide for the Removal of 17 $\alpha$ -Ethinylestradiol (EE2). *Water Res.* **2004**, *38* (1), 184–192.
- (71) Forrez, I.; Carballa, M.; Noppe, H.; De Brabander, H.; Boon, N.; Verstraete, W. Influence of Manganese and Ammonium Oxidation on the Removal of 17 $\alpha$ -Ethinylestradiol (EE2). *Water Res.* **2009**, *43* (1), 77–86.
- (72) Xiao, X. Degradation of Emerging Contaminants by Fe- and Mn- Based Oxidation Methods in Aqueous Solution. *PhD diss. Cornell University.* **2012**, (7).
- (73) Banh, A.; Chavez, V.; Doi, J.; Nguyen, A.; Hernandez, S.; Ha, V.; Jimenez, P.; Espinoza, F.; Johnson, H. A. Manganese (Mn) Oxidation Increases Intracellular Mn in *Pseudomonas Putida* GB-1. *PLoS One* **2013**, *8* (10), 1–8.
- (74) Estes, E. R.; Andeer, P. F.; Nordlund, D.; Wankel, S. D.; Hansel, C. M. Biogenic Manganese Oxides as Reservoirs of Organic Carbon and Proteins in Terrestrial and Marine Environments. *Geobiology* **2017**, *15* (1), 158–172.
- (75) Kolvenbach, B.; Schlaich, N.; Raoui, Z.; Prell, J.; Zühlke, S.; Schäffer, A.; Guengerich, F. P.; Corvini, P. F. X. Degradation Pathway of Bisphenol A: Does Ipso Substitution Apply to Phenols Containing a Quaternary  $\alpha$ -Carbon Structure in the Para Position? *Appl. Environ. Microbiol.* **2007**, *73* (15), 4776–4784.
- (76) Krumbein, W. E.; Altmann, H. J. A New Method for the Detection and Enumeration of Manganese Oxidizing and Reducing Microorganisms. *Helgoländer Wissenschaftliche Meeresuntersuchungen* **1973**, *25* (2–3), 347–356.

- (77) Endo, Y.; Kimura, N.; Ikeda, I.; Fujimoto, K.; Kimoto, H. Adsorption of Bisphenol A by Lactic Acid Bacteria, *Lactococcus*, Strains. *Appl. Microbiol. Biotechnol.* **2007**, *74* (1), 202–207.
- (78) Im, J.; Yip, D.; Lee, J.; Löffler, F. E. Simplified Extraction of Bisphenols from Bacterial Culture Suspensions and Solid Matrices. *J. Microbiol. Methods* **2016**, *126*, 35–37.
- (79) Tebo B, Clement B, Dick G. Biotransformations of Manganese. *Manual of Environ. Microbiol.* **2007**. (3), 1223-1238.
- (80) Tebo, B. M.; Johnson, H. A.; McCarthy, J. K.; Templeton, A. S. Geomicrobiology of Manganese(II) Oxidation. *Trends Microbiol.* **2005**, *13* (9), 421–428.
- (81) Villalobos, M.; Toner, B.; Bargar, J.; Sposito, G. Characterization of the Manganese Oxide Produced by *Pseudomonas Putida* Strain MnB1. *Geochim. Cosmochim. Acta* **2003**, *67* (14), 2649–2662.
- (82) Hansel, C. M.; Francis, C. A. Coupled Photochemical and Enzymatic Mn(II) Oxidation Pathways of a Planktonic Roseobacter-like Bacterium. *Appl. Environ. Microbiol.* **2006**, *72* (5), 3543–3549.
- (83) Okazaki, M.; Sugita, T.; Shimizu, M.; Ohode, Y.; Iwamoto, K.; De Vrind-de Jong, E. W.; De Vrind, J. P. M.; Corstjens, P. L. A. M. Partial Purification and Characterization of Manganese-Oxidizing Factors of *Pseudomonas Fluorescens* GB-1. *Appl. Environ. Microbiol.* **1997**, *63* (12), 4793–4799.
- (84) Sasaki, M.; Maki, J. I.; Oshiman, K. I.; Matsumura, Y.; Tsuchido, T. Biodegradation of Bisphenol A by Cells and Cell Lysate from *Sphingomonas* Sp. Strain AO1. *Biodegradation* **2005**, *16* (5), 449–459.
- (85) Fischer, J.; Kappelmeyer, U.; Kastner, M.; Schauer, F.; Heipieper, H. J. The Degradation of Bisphenol A by the Newly Isolated Bacterium *Cupriavidus Basiliensis* JF1 Can Be Enhanced by Biostimulation with Phenol. *Int. Biodeterior. Biodegrad.* **2010**, *64* (4), 324–330.

- (86) Ghiorse, W. C. Biology of Iron- and Manganese-Depositing Bacteria. *Annu. Rev. Microbiol.* **1984**, *38* (1), 515–550.
- (87) Forrez, I.; Carballa, M.; Fink, G.; Wick, A.; Hennebel, T.; Vanhaecke, L.; Ternes, T.; Boon, N.; Verstraete, W. Biogenic Metals for the Oxidative and Reductive Removal of Pharmaceuticals, Biocides and Iodinated Contrast Media in a Polishing Membrane Bioreactor. *Water Res.* **2011**, *45* (4), 1763–1773.
- (88) Heemken, O. P.; Reincke, H.; Stachel, B.; Theobald, N. The Occurrence of Xenoestrogens in the Elbe River and the North Sea. *Chemosphere* **2001**, *45* (3), 245–259.
- (89) Wagner-Döbler, I.; Biebl, H. Environmental Biology of the Marine Roseobacter Lineage. *Annu. Rev. Microbiol.* **2006**, *60*, 255–280.
- (90) Buchan, A.; González, J. M.; Moran, M. A. Overview of the Marine Roseobacter Lineage. *Appl. Environ. Microbiol.* **2005**, *71* (10), 5665–5677.
- (91) Ying, G. G.; Kookana, R. S. Degradation of Five Selected Endocrine-Disrupting Chemicals in Seawater and Marine Sediment. *Environ. Sci. Technol.* **2003**, *37* (7), 1256–1260.
- (92) Davies, G. Some Aspects of the Chemistry of Manganese(III) in Aqueous Solution. *Coord. Chem. Rev.* **1969**, *4* (2), 199–224.
- (93) McKenzie, R. M. The Synthesis of Birnessite, Cryptomelane, and Some Other Oxides and Hydroxides of Manganese. *Mineral. Mag.* **1971**, *38* (296), 493–502.
- (94) Ling, F. T.; Heaney, P. J.; Post, J. E.; Gao, X. Transformations from Triclinic to Hexagonal Birnessite at Circumneutral PH Induced through PH Control by Common Biological Buffers. *Chem. Geol.* **2015**, *416*, 1–10.
- (95) Templeton, A. S.; Staudigel, H.; Tebo, B. M. Diverse Mn(II)-Oxidizing Bacteria Isolated from Submarine Basalts at Loihi Seamount. *Geomicrobiol. J.* **2005**, *22* (3–4), 127–139.

- (96) Liu, W.; Sun, B.; Qiao, J.; Guan, X. Influence of Pyrophosphate on the Generation of Soluble Mn(III) from Reactions Involving Mn Oxides and Mn(VII). *Environ. Sci. Technol.* **2019**, *53* (17), 10227–10235.
- (97) Gao, Y.; Jiang, J.; Zhou, Y.; Pang, S. Y.; Jiang, C.; Guo, Q.; Duan, J. Bin. Does Soluble Mn(III) Oxidant Formed in Situ Account for Enhanced Transformation of Triclosan by Mn(VII) in the Presence of Ligands? *Environ. Sci. Technol.* **2018**, *52* (8), 4785–4793.
- (98) Webb, S. M.; Tebo, B. M.; Bargar, J. R. Structural Characterization of Biogenic Mn Oxides Produced in Seawater by the Marine *Bacillus* Sp. Strain SG-1. *Am. Mineral.* **2005**, *90* (8–9), 1342–1357.
- (99) Silvester, E.; Manceau, A.; Drits, V. A. Structure of Synthetic Monoclinic Na-Rich Birnessite and Hexagonal Birnessite: II. Results from Chemical Studies and EXAFS Spectroscopy. *Am. Mineral.* **1997**, *82* (9–10), 962–978.
- (100) Lanson, B.; Drits, V. A.; Silvester, E.; Manceau, A. Structure of H-Exchanged Hexagonal Birnessite and Its Mechanism of Formation from Na-Rich Monoclinic Buserite at Low PH. *Am. Mineral.* **2000**, *85* (5–6), 826–838.
- (101) Xu, L.; Xu, C.; Zhao, M.; Qiu, Y.; Sheng, G. D. Oxidative Removal of Aqueous Steroid Estrogens by Manganese Oxides. *Water Res.* **2008**, *42* (20), 5038–5044.
- (102) Lanson, B.; Drits, V. A.; Feng, Q.; Manceau, A. Structure of Synthetic Na-Birnessite: Evidence for a Triclinic One-Layer Unit Cell. *Am. Mineral.* **2002**, *87* (11–12), 1662–1671.
- (103) Bolz, U.; Hagenmaier, H.; Körner, W. Phenolic Xenoestrogens in Surface Water, Sediments, and Sewage Sludge from Baden-Württemberg, South-West Germany. *Environ. Pollut.* **2001**, *115* (2), 291–301.
- (106) Kostka, J. E.; Nealson, K. Isolation, cultivation and characterization of iron- and manganese-reducing bacteria. *In Techniques in microbial ecology.* **1998**, 468.
- (107) *National Center for Biotechnology Information.* **2019.**